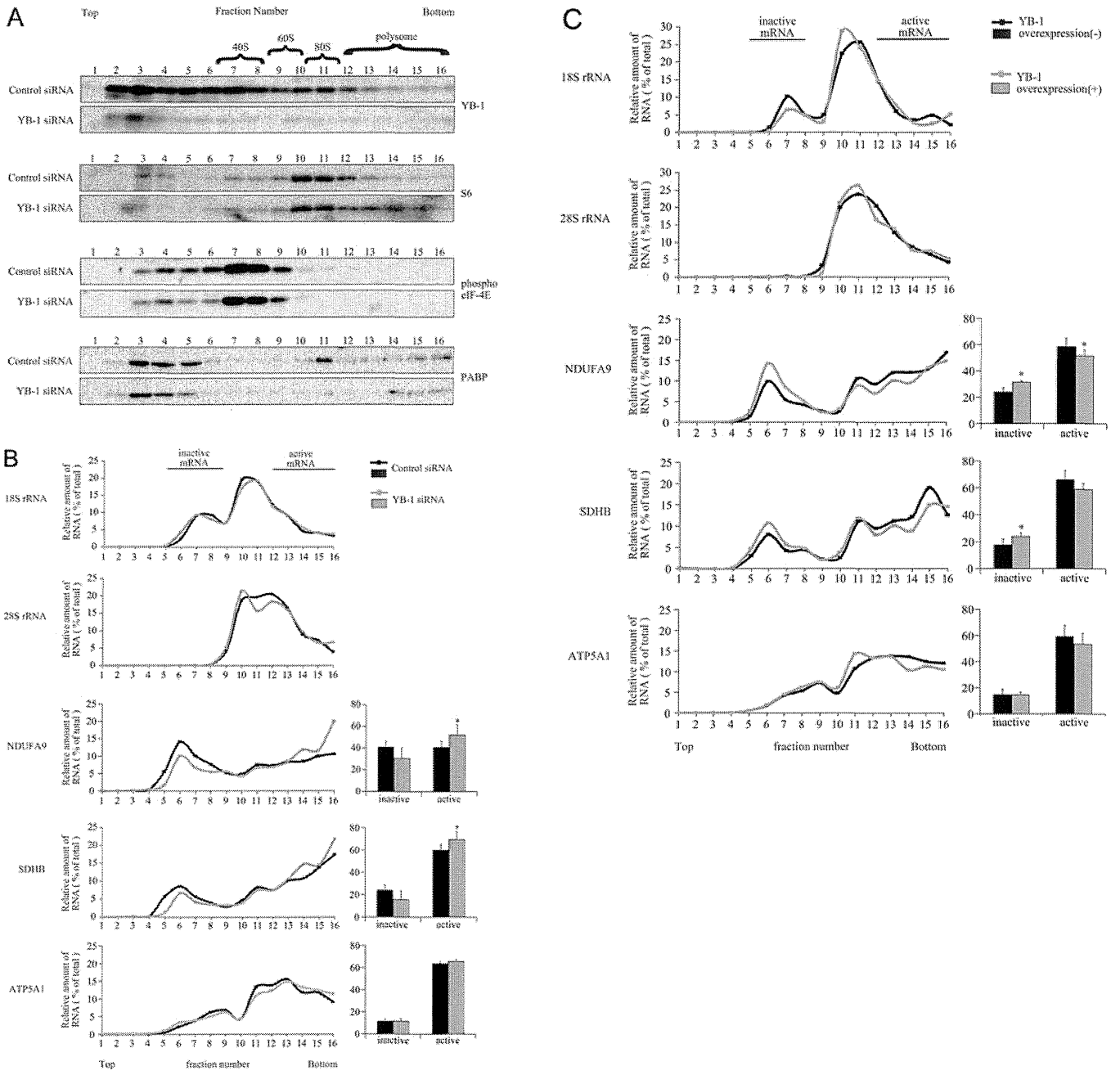

Figure 5 YB-1 regulates the recruitment of mRNAs from mRNPs to polysomes

(**A**) Cell lysates were prepared from HeLa cells treated with YB-1 or control siRNA for 72 h. The post-nuclear supernatant was layered over a 15–45% (w/v) sucrose gradient and separated by centrifugation. A total of 16 fractions were collected. The protein levels in each fraction were analysed by immunoblotting. 40S, 60S and 80S monosome, and polysome, fraction was defined by the distribution of 18S and 28S rRNAs. (**B**) The mRNA levels in each fraction were determined by qRT–PCR with specific primers for 18S rRNA, 28S rRNA, NDUFA9, SDHB and ATP5A1. The mRNAs in fractions 5–9 were classified as translationally inactive mRNAs, whereas those in fractions 12–16 were classified as active mRNAs. (**C**) YB-1–HA was overexpressed by adding doxycycline for 48 h. Sucrose gradient centrifugation was performed with induced or non-induced cells as described for (**A**). The RNA levels in each fraction were analysed by qRT–PCR. The results shown were obtained from three independent experiments and shown as means ± S.D. $^*P < 0.05$ by Student's t test.

In contrast with YB-1 depletion, YB-1 overexpression led to increases in *NDUFA9* and *SDHB* mRNAs in fractions 5–8 and decreases in fractions 12–16, indicating that the inactive mRNAs were increased and the active mRNAs were decreased (Figure 5C). The distribution of *ATP5A1* mRNA was not altered by YB-1 overexpression. In this overexpression experiment (Figure 5C) compared with YB-1 depletion (Figure 5B), we observed the different distribution of mRNA in control points because of different cell lines and different serum conditions. These findings suggest that YB-1 regulates the recruitment of the target mRNAs from mRNPs to polysomes by the quantity of YB-1.

Depletion of YB-1 leads to up-regulation of mitochondrial function

The mitochondrial respiratory chain is formed co-operatively by proteins encoded in the nucleus and mitochondria. The YB-1 siRNA-mediated elevation of the nuclear-encoded OXPHOS

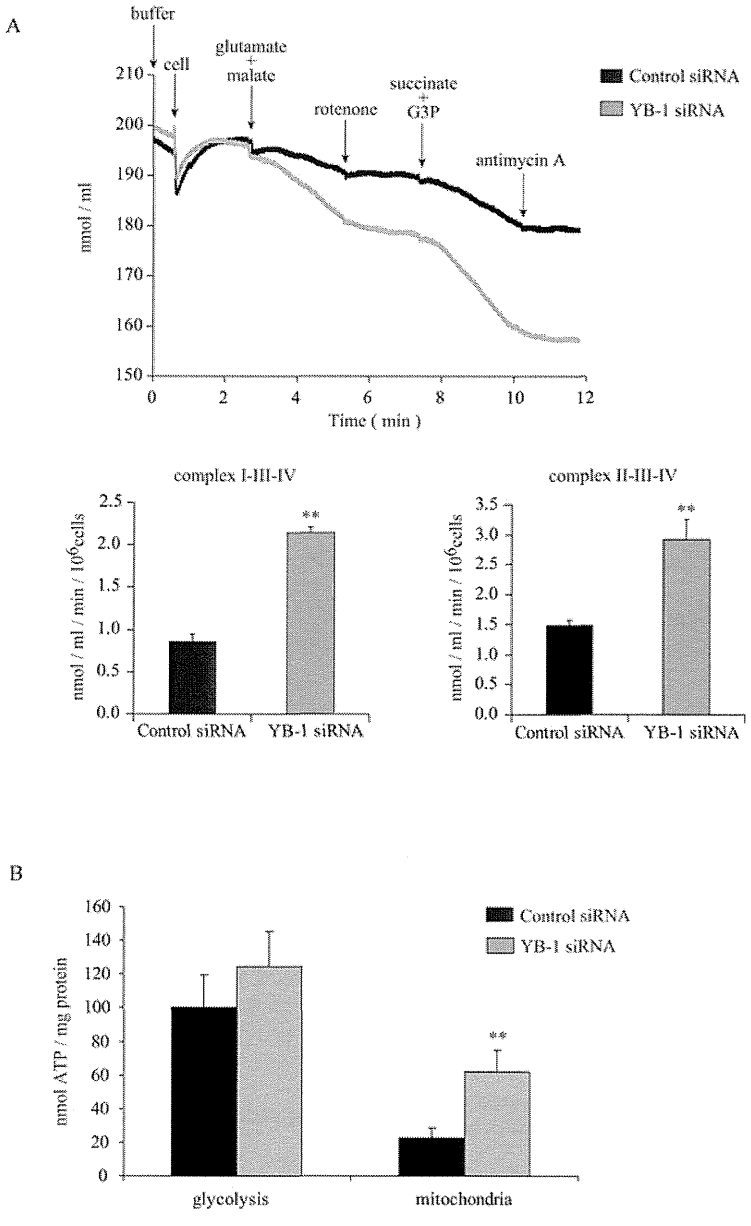

Figure 6 Depletion of YB-1 affects mitochondrial OXPHOS activity

(**A**) HeLa cells treated with a control or YB-1 siRNA for 72 h were permeabilized using 1 % (w/v) digitonin. Oxygen consumption was measured using a Clark-type electrode. The glutamate and malate respiration depended on the activities of complex I-III-IV. The succinate and G3P respiration depended on the activities of complex II-III-IV. (**B**) At 72 h after siRNA transfection, the cells were lysed and the glycolytic and mitochondrial ATP levels were measured using chemiluminescence. The results shown were obtained from three independent experiments and are means ± S.D. $^{**}P < 0.01$ by Student's *t* test.

proteins may influence mitochondrial functions. First, we measured oxygen consumption using a Clark-type oxygen electrode. We defined oxygen consumption when cells were treated with glutamate and malate as the electron flow at complex I-III-IV and that when succinate and G3P were added to rotenone-treated cells as the electron flow at complex II-III-IV. YB-1 depletion increased the electron flows at both complex I-III-IV and complex II-III-IV by approximately 2-fold (Figure 6A). Next, we measured the ATP levels. YB-1 depletion increased mitochondrial ATP by 3-fold, but not glycolytic ATP (Figure 6B). These findings suggest that YB-1 controls mitochondrial function by regulating the expression of nuclear-encoded OXPHOS proteins.

YB-1 associates with PABP [poly(A)-binding protein] through mRNAs

YB-1 is phosphorylated by the serine/threonine kinase Akt [20]. We confirmed that YB-1 was phosphorylated at Ser^{102} in response to growth stimuli such as IGF-I and 20 % (v/v) FBS. Phosphorylated YB-1 was already detected after 1 h of stimulation (Figure 7A, lanes 2 and 5), and then dropped again after 12 h (Figure 7A, lanes 4 and 7). These findings suggest that YB-1 becomes transiently phosphorylated and dephosphorylated at Ser^{102}.

YB-1 is a component of stress granules [30] and P-bodies (processing bodies) [31]. We investigated whether YB-1

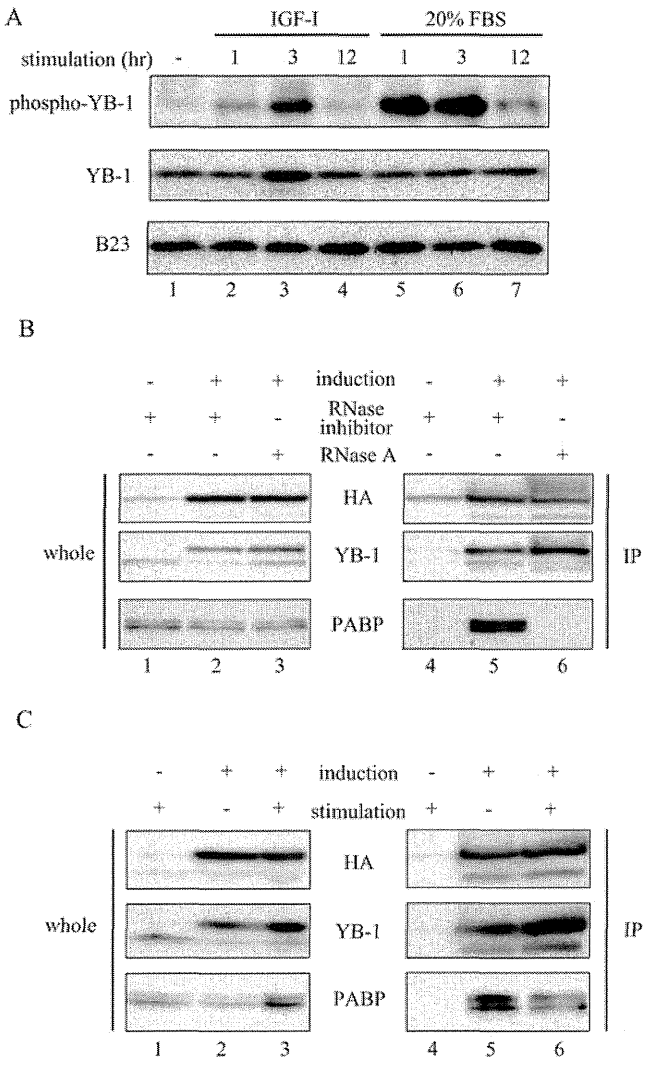

Figure 7 YB-1 associates with the proteins in stress granules and P-bodies through mRNAs and the associations are lost after YB-1 phosphorylation

(**A**) HeLa cells were cultured in serum-free medium for 24 h and stimulated by 50 ng/ml IGF-I or 20% (v/v) FBS for the last few hours as indicated. The protein levels were detected by immunoblotting with antibodies against phospho-YB-1 (Ser^{102}) and YB-1. (**B**) YB-1–HA overexpression was induced by doxycycline for 48 h. The cells were lysed in a buffer containing 200 units/ml RNase inhibitor or 100 μg/ml RNase A and subjected to immunoprecipitation using anti-HA agarose beads. The immunoprecipitated proteins (IP) and whole cell lysates were analysed by immunoblotting with antibodies against the indicated proteins. PABP is a marker for polysomes. (**C**) YB-1–HA-overexpressing cells induced for 48 h were cultured in serum-free medium for 24 h and stimulated by 20% (v/v) FBS for the last 6 h. Cell lysates (whole) were subjected to immunoprecipitation with anti-HA agarose beads. The immunoprecipitated proteins (IP) were detected by immunoblotting with antibodies against the indicated proteins.

interacted with proteins contained in these components. Co-immunoprecipitation assays revealed that YB-1 associated with PABP concentrated in stress granules in the cytoplasm (Figure 7B) [28]. The associations were abolished by RNase treatment (Figure 7B, lanes 5 and 6), suggesting that YB-1 associated with PABP mRNAs.

Phosphorylated YB-1 disengages from the capped 5′-termini of mRNAs and fails to inhibit their translation [19]. To confirm whether phosphorylated YB-1 was released from mRNAs, we assessed the amount of PABP interacting with YB-1 after serum stimulation, since PABP associated with YB-1 through mRNAs (Figure 7B). A co-immunoprecipitation assay revealed that the association between YB-1 and PABP was attenuated after serum stimulation (Figure 7C, lanes 5 and 6), suggesting that the amount of PABP bound to mRNA decreases as a result of the increasing amount of YB-1 which competes with PABP for binding to mRNA.

The increases in the nuclear-encoded proteins in response to serum stimulation mediate the translational regulation by YB-1

In the present study, we observed that serum stimulation regulated the expression of nuclear-encoded OXPHOS proteins in a translation-dependent manner (Figure 2) and led to phosphorylation of the translational regulator YB-1 (Figure 7A), and that YB-1 overexpression suppressed the expression of OXPHOS proteins such as NDUFA9 up-regulated by serum stimulation (Figure 4). We therefore hypothesized that the translational regulation in response to serum stimulation was mediated by YB-1. We investigated whether the serum stimulation-induced expressions of OXPHOS proteins were suppressed by YB-1 overexpression. NDUFA9 and UQCRFS1 proteins were increased by approximately 30% in response to serum stimulation in non-overexpressing cells, and YB-1 overexpression cancelled these elevations of expression in response to serum stimulation. On the other hand, SDHA, ATP5A1 and B23 showed no change regardless of the amount of YB-1 (Figures 8A and 8B). These findings suggest that overexpressed YB-1 bound to mRNAs excessively and suppressed their translation, such that the reaction to serum stimulation was only attenuated in mRNAs whose translation was regulated by YB-1.

Next, we examined the effects of YB-1 overexpression on the changes in the ATP level in response to serum stimulation. Mitochondrial ATP was increased by approximately 2.7-fold in response to serum stimulation in non-overexpressing cells, and the change was suppressed by 1.7-fold in YB-1-overexpressing cells (Figure 8C). It is probable that the mitochondrial ATP production in response to serum stimulation was weakened because of decreased protein expression.

DISCUSSION

We have shown that YB-1 is essential for mitochondrial OXPHOS activity, on the basis of the following evidence: (i) serum stimulation up-regulated nuclear-encoded OXPHOS proteins and mitochondrial ATP production in a translation-dependent manner; (ii) YB-1 depletion led to up-regulation of mitochondrial function through induction of OXPHOS protein translation from mRNP release; and (iii) YB-1 overexpression suppressed the translation of these OXPHOS mRNAs because of reduced polysome formation. These findings suggest that the major ribonucleoprotein YB-1 is a critical factor for translation that may control OXPHOS protein translation.

Lithgow et al. [32] suggested that RNA-binding proteins could coat mRNAs in the nucleus, leading to mRNP formation and export to the cytoplasm to ensure translational repression during transport. Directed transport of mRNAs out of the nucleus, following a cytoplasmic pathway to a specified organelle in the cytoplasm, may also contribute to the fidelity of protein targeting observed in all eukaryotic cells [32]. These observations suggested that site-specific mRNA translation may be important for precise control of both the localization and the rate of co-translational protein import into mitochondria. The primary function of mitochondria is ATP production via the OXPHOS pathway and the mtDNA molecule only encodes 13 proteins that are members of the respiratory chain. In the present

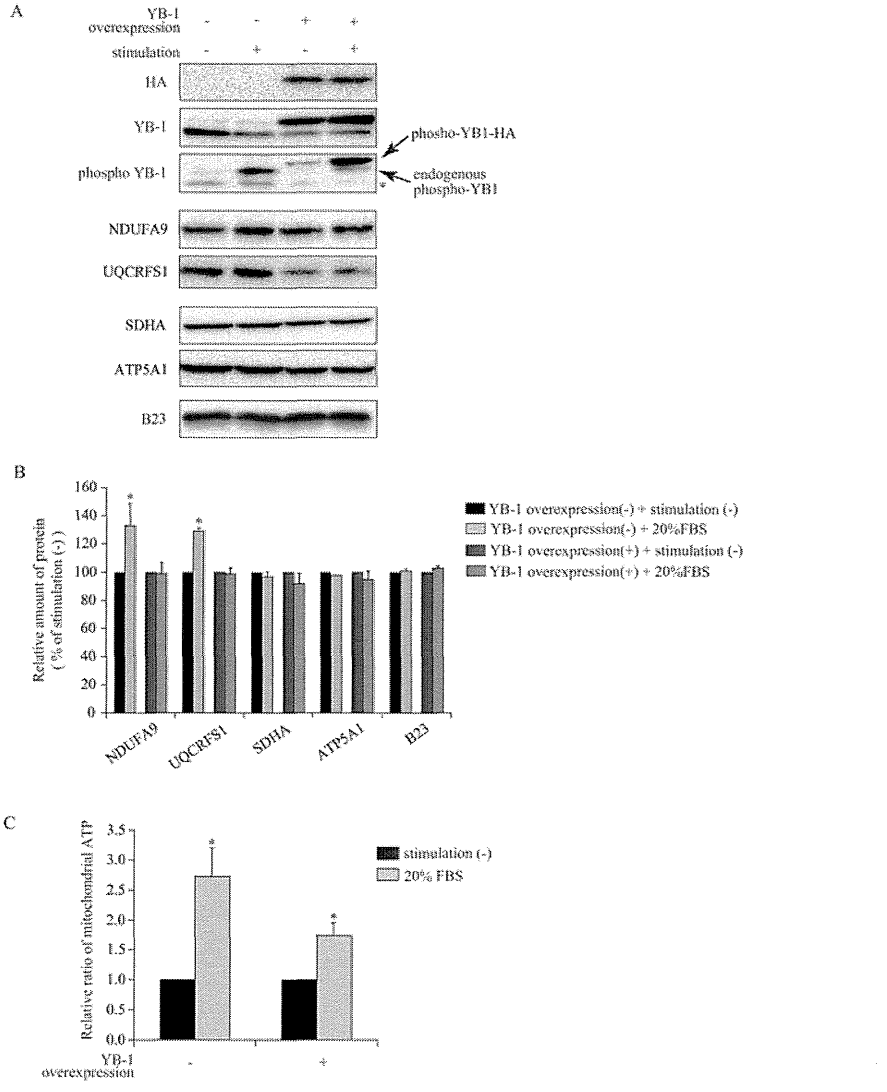

Figure 8 YB-1 overexpression attenuates the up-regulation of mitochondrial function in response to serum stimuli

(**A**) Overexpression of YB-1–HA was induced by doxycycline for 48 h. The cells were cultured in serum-free media for 18 h and then stimulated with 20% (v/v) FBS for the last 6 h. Western blotting was performed using antibodies against the indicated proteins. The asterisk indicates a non-specific band. (**B**) The intensities of the signals in (**A**) were analysed by densitometry. (**C**) The mitochondrial ATP levels were measured using chemiluminescence in YB-1–HA-overexpressing cells stimulated by 20% (v/v) FBS for 6 h. The results shown were obtained from three independent experiments and are means ± S.D. $^*P < 0.05$ by Student's *t* test.

study, we focused on OXPHOS protein translation, analysed the associations of several cytosolic mRNAs and examined which RNA-binding proteins were involved in translational control under serum stimulation with regard to OXPHOS mRNAs.

The transcriptional regulation of nuclear genes encoding mitochondria-localized proteins is certainly important, but it cannot account for the fast adaptive response. A previous study has underscored the importance of a co-translational import process involving a large set of proteins for mitochondrial biogenesis [33]. This process, which relies on the tight translational regulation of localized mRNAs, can rapidly respond to cellular conditions while allowing the possibility of orchestrating complex assembly at discrete foci on the mitochondrial membrane.

YB-1-bound mRNAs were identified using immunoprecipitation microarray analyses and *UQCRC1*, whose protein is a part of respiratory complex III and is in the list of the top 100 immunoprecipitation-enriched genes [34]. We identified *UQCRC1* mRNAs as YB-1-bound mRNAs using immunoprecipitation analyses, suggesting that our immunoprecipitation experiments were reliable.

The most substantial mechanism by which YB-1 controls cell growth is via its influence on cytoplasmic translation. In the presence of nutrients, YB-1 not only greatly promotes the production of new ribosomes, but also increases translation from existing ribosomes. However, the issues of whether and how YB-1 regulates mitochondrial translation have not been addressed. YB-1 is a major constituent of translationally inactive mRNPs [35] and is also present in active polysomes [27,36]. YB-1 appears to exert a concentration-dependent effect on global translation. Low YB-1/mRNA ratios typical for polysomal mRNAs may result in translational stimulation, whereas high ratios are typical for translationally repressed mRNAs [15] and result in translational inhibition by displacement of the translation initiation factor eIF-4G [19,36]. In the present study, we observed that YB-1 was phosphorylated at Ser^{102} after serum stimulation, probably through PI3K, and released from

mRNA complexes to active ribosomes to increase translation (Figure 7).

The PI3K/Akt signalling pathway leads to the TOR (target of rapamycin) pathway. Although inhibition of the TOR pathway leads to a global decrease in cytoplasmic translation [38], *tor1*-null cells exhibit a higher rate of mitochondrial translation and increases in the expressions of several mitochondrial-encoded OXPHOS components [39]. This connection between TOR activity and membrane-linked translation may be an important aspect of mitochondrial import regulation, since many mRNAs encoding mitochondrial proteins are translated by ribosomes present at the external membrane of mitochondria. These observations suggest that mTOR signalling could be a key player in the regulation of the mitochondrial import process and mitochondrial biogenesis. YB-1 is also regulated by the PI3K/Akt/mTOR pathway.

YB-1 may serve as a regulatory signal in processes taking place in P-bodies. YB-1–mRNA complexes can be stored in P-bodies where they are translationally silenced and either degraded or released back in the translating pool [40]. Growth factors increase the translation of nuclear-encoded mitochondrial OXPHOS genes, leading to alterations in P-body-linked YB-1 properties [41], and may favour the formation of co-translationally active mRNA–YB-1-mitochondria complexes. In the present study, we did not observe that YB-1 was localized in P-bodies in sucrose gradient analyses. This model is speculative; many of the factors involved in this equilibrium remain to be studied, and could therefore control the localization and translation/degradation balance of the target mRNAs. In the present study, we observed that YB-1 regulated the translation of mitochondrial OXPHOS mRNAs through mRNA binding for mitochondrial function.

AUTHOR CONTRIBUTION

Shinya Matsumoto designed experiments, conducted experiments, analysed data and wrote the paper. Takeshi Uchiumi designed experiments, analysed data and wrote the paper. Hiroyuki Tanamachi, Toshiro Saito, Mikako Yagi and Shinya Takazaki conducted experiments and analysed data. Tomotake Kanki designed experiments, analysed data and wrote the paper. Dongchon Kang designed experiments and wrote the paper.

ACKNOWLEDGEMENTS

We acknowledge the technical expertise of the Support Center for Education and Research, Kyushu University.

FUNDING

This work was supported in part by Grants-in-Aid for Scientific Research from the Ministry of Education, Science, Technology, Sports and Culture of Japan [grant numbers 19209019 and 21590337].

REFERENCES

1 Anderson, S., Bankier, A. T., Barrell, B. G., de Bruijn, M. H., Coulson, A. R., Drouin, J., Eperon, I. C., Nierlich, D. P., Roe, B. A., Sanger, F. et al. (1981) Sequence and organization of the human mitochondrial genome. Nature **290**, 457–465
2 Kang, D. and Hamasaki, N. (2005) Mitochondrial transcription factor A in the maintenance of mitochondrial DNA: overview of its multiple roles. Ann. NY Acad. Sci. **1042**, 101–108
3 Neupert, W. (1997) Protein import into mitochondria. Annu. Rev. Biochem. **66**, 863–917
4 Bolender, N., Sickmann, A., Wagner, R., Meisinger, C. and Pfanner, N. (2008) Multiple pathways for sorting mitochondrial precursor proteins. EMBO Rep. **9**, 42–49
5 Ades, I. Z. and Butow, R. A. (1980) The products of mitochondria-bound cytoplasmic polysomes in yeast. J. Biol. Chem. **255**, 9918–9924
6 Funfschilling, U. and Rospert, S. (1999) Nascent polypeptide-associated complex stimulates protein import into yeast mitochondria. Mol. Biol. Cell. **10**, 3289–3299
7 Kenmochi, N., Suzuki, T., Uechi, T., Magoori, M., Kuniba, M., Higa, S., Watanabe, K. and Tanaka, T. (2001) The human mitochondrial ribosomal protein genes: mapping of 54 genes to the chromosomes and implications for human disorders. Genomics **77**, 65–70
8 Dugre-Brisson, S., Elvira, G., Boulay, K., Chatel-Chaix, L., Mouland, A. J. and DesGroseillers, L. (2005) Interaction of Staufen1 with the 5′ end of mRNA facilitates translation of these RNAs. Nucleic Acids Res. **33**, 4797–4812
9 Skabkina, O. V., Skabkin, M. A., Popova, N. V., Lyabin, D. N., Penalva, L. O. and Ovchinnikov, L. P. (2003) Poly(A)-binding protein positively affects YB-1 mRNA translation through specific interaction with YB-1 mRNA. J. Biol. Chem. **278**, 18191–18198
10 Kohno, K., Izumi, H., Uchiumi, T., Ashizuka, M. and Kuwano, M. (2003) The pleiotropic functions of the Y-box-binding protein, YB-1. Bioessays **25**, 691–698
11 Matsumoto, K. and Wolffe, A. P. (1998) Gene regulation by Y-box proteins: coupling control of transcription and translation. Trends Cell Biol. **8**, 318–323
12 Ashizuka, M., Fukuda, T., Nakamura, T., Shirasuna, K., Iwai, K., Izumi, H., Kohno, K., Kuwano, M. and Uchiumi, T. (2002) Novel translational control through an iron-responsive element by interaction of multifunctional protein YB-1 and IRP2. Mol. Cell. Biol. **22**, 6375–6383
13 Fukuda, T., Ashizuka, M., Nakamura, T., Shibahara, K., Maeda, K., Izumi, H., Kohno, K., Kuwano, M. and Uchiumi, T. (2004) Characterization of the 5′-untranslated region of YB-1 mRNA and autoregulation of translation by YB-1 protein. Nucleic Acids Res. **32**, 611–622
14 Evdokimova, V. M. and Ovchinnikov, L. P. (1999) Translational regulation by Y-box transcription factor: involvement of the major mRNA-associated protein, p50. Int. J. Biochem. Cell Biol. **31**, 139–149
15 Skabkin, M. A., Kiselyova, O. I., Chernov, K. G., Sorokin, A. V., Dubrovin, E. V., Yaminsky, I. V., Vasiliev, V. D. and Ovchinnikov, L. P. (2004) Structural organization of mRNA complexes with major core mRNP protein YB-1. Nucleic Acids Res. **32**, 5621–5635
16 Lu, Z. H., Books, J. T. and Ley, T. J. (2005) YB-1 is important for late-stage embryonic development, optimal cellular stress responses, and the prevention of premature senescence. Mol. Cell. Biol. **25**, 4625–4637
17 Uchiumi, T., Fotovati, A., Sasaguri, T., Shibahara, K., Shimada, T., Fukuda, T., Nakamura, T., Izumi, H., Tsuzuki, T., Kuwano, M. and Kohno, K. (2006) YB-1 is important for an early stage embryonic development: neural tube formation and cell proliferation. J. Biol. Chem. **281**, 40440–40449
18 Bader, A. G., Felts, K. A., Jiang, N., Chang, H. W. and Vogt, P. K. (2003) Y box-binding protein 1 induces resistance to oncogenic transformation by the phosphatidylinositol 3-kinase pathway. Proc. Natl. Acad. Sci. U.S.A. **100**, 12384–12389
19 Evdokimova, V., Ruzanov, P., Anglesio, M. S., Sorokin, A. V., Ovchinnikov, L. P., Buckley, J., Triche, T. J., Sonenberg, N. and Sorensen, P. H. (2006) Akt-mediated YB-1 phosphorylation activates translation of silent mRNA species. Mol. Cell. Biol. **26**, 277–292
20 Sutherland, B. W., Kucab, J., Wu, J., Lee, C., Cheang, M. C., Yorida, E., Turbin, D., Dedhar, S., Nelson, C., Pollak, M. et al. (2005) Akt phosphorylates the Y-box binding protein 1 at Ser102 located in the cold shock domain and affects the anchorage-independent growth of breast cancer cells. Oncogene **24**, 4281–4292
21 Rajasekhar, V. K., Viale, A., Socci, N. D., Wiedmann, M., Hu, X. and Holland, E. C. (2003) Oncogenic Ras and Akt signaling contribute to glioblastoma formation by differential recruitment of existing mRNAs to polysomes. Mol. Cell **12**, 889–901
22 Unterluggauer, H., Hutter, E., Viertler, H. P. and Jansen-Durr, P. (2008) Insulin-like growth factor-induced signals activate mitochondrial respiration. Biotechnol. J. **3**, 813–816
23 Shibahara, K., Uchiumi, T., Fukuda, T., Kura, S., Tominaga, Y., Maehara, Y., Kohno, K., Nakabeppu, Y., Tsuzuki, T. and Kuwano, M. (2004) Targeted disruption of one allele of the Y-box binding protein-1 (YB-1) gene in mouse embryonic stem cells and increased sensitivity to cisplatin and mitomycin C. Cancer Sci. **95**, 348–353
24 Ohgaki, K., Kanki, T., Fukuoh, A., Kurisaki, H., Aoki, Y., Ikeuchi, M., Kim, S. H., Hamasaki, N. and Kang, D. (2007) The C-terminal tail of mitochondrial transcription factor A markedly strengthens its general binding to DNA. J. Biochem. **141**, 201–211
25 Claypool, S. M., Oktay, Y., Boontheung, P., Loo, J. A. and Koehler, C. M. (2008) Cardiolipin defines the interactome of the major ADP/ATP carrier protein of the mitochondrial inner membrane. J. Cell Biol. **182**, 937–950
26 Hofhaus, G., Shakeley, R. M. and Attardi, G. (1996) Use of polarography to detect respiration defects in cell cultures. Methods Enzymol. **264**, 476–483
27 Evdokimova, V. M., Kovrigina, E. A., Nashchekin, D. V., Davydova, E. K., Hershey, J. W. and Ovchinnikov, L. P. (1998) The major core protein of messenger ribonucleoprotein particles (p50) promotes initiation of protein biosynthesis *in vitro*. J. Biol. Chem. **273**, 3574–3581
28 Buchan, J. R. and Parker, R. (2009) Eukaryotic stress granules: the ins and outs of translation. Mol. Cell **36**, 932–941
29 Cataldo, L., Mastrangelo, M. A. and Kleene, K. C. (1999) A quantitative sucrose gradient analysis of the translational activity of 18 mRNA species in testes from adult mice. Mol. Hum. Reprod. **5**, 206–213

30 Onishi, H., Kino, Y., Morita, T., Futai, E., Sasagawa, N. and Ishiura, S. (2008) MBNL1 associates with YB-1 in cytoplasmic stress granules. J. Neurosci. Res. **86**, 1994–2002
31 Yang, W. H. and Bloch, D. B. (2007) Probing the mRNA processing body using protein macroarrays and "autoantigenomics". RNA **13**, 704–712
32 Lithgow, T., Cuezva, J. M. and Silver, P. A. (1997) Highways for protein delivery to the mitochondria. Trends Biochem. Sci. **22**, 110–113
33 Garcia, M., Darzacq, X., Delaveau, T., Jourdren, L., Singer, R. H. and Lacq, C. (2007) Mitochondria-associated yeast mRNAs and the biogenesis of molecular complexes. Mol. Biol. Cell **18**, 362–368
34 Dong, J., Akcakanat, A., Stivers, D. N., Zhang, J., Kim, D. and Meric-Bernstam, F. (2009) RNA-binding specificity of Y-box protein 1. RNA Biol. **6**, 59–64
35 Evdokimova, V., Ruzanov, P., Imataka, H., Raught, B., Svitkin, Y., Ovchinnikov, L. P. and Sonenberg, N. (2001) The major mRNA-associated protein YB-1 is a potent 5′ cap-dependent mRNA stabilizer. EMBO J. **20**, 5491–5502
36 Minich, W. B. and Ovchinnikov, L. P. (1992) Role of cytoplasmic mRNP proteins in translation. Biochimie **74**, 477–483
37 Nekrasov, M. P., Ivshina, M. P., Chernov, K. G., Kovrigina, E. A., Evdokimova, V. M., Thomas, A. A., Hershey, J. W. and Ovchinnikov, L. P. (2003) The mRNA-binding protein YB-1 (p50) prevents association of the eukaryotic initiation factor eIF4G with mRNA and inhibits protein synthesis at the initiation stage. J. Biol. Chem. **278**, 13936–13943
38 Schmelzle, T. and Hall, M. N. (2000) TOR, a central controller of cell growth. Cell **103**, 253–262
39 Bonawitz, N. D., Chatenay-Lapointe, M., Pan, Y. and Shadel, G. S. (2007) Reduced TOR signaling extends chronological life span via increased respiration and upregulation of mitochondrial gene expression. Cell Metab. **5**, 265–277
40 Brengues, M., Teixeira, D. and Parker, R. (2005) Movement of eukaryotic mRNAs between polysomes and cytoplasmic processing bodies. Science **310**, 486–489
41 Foat, B. C., Houshmandi, S. S., Olivas, W. M. and Bussemaker, H. J. (2005) Profiling condition-specific, genome-wide regulation of mRNA stability in yeast. Proc. Natl. Acad. Sci. U.S.A. **102**, 17675–17680

Received 3 October 2011/5 January 2012; accepted 27 January 2012
Published as BJ Immediate Publication 27 January 2012, doi:10.1042/BJ20111728

Biochem. J. (2012) **443**, 573–584 (Printed in Great Britain) doi:10.1042/BJ20111728

online data

SUPPLEMENTARY ONLINE DATA

Ribonucleoprotein Y-box-binding protein-1 regulates mitochondrial oxidative phosphorylation (OXPHOS) protein expression after serum stimulation through binding to OXPHOS mRNA

Shinya MATSUMOTO, Takeshi UCHIUMI[1], Hiroyuki TANAMACHI, Toshiro SAITO, Mikako YAGI, Shinya TAKAZAKI, Tomotake KANKI and Dongchon KANG

Department of Clinical Chemistry and Laboratory Medicine, Graduate School of Medical Sciences, Kyushu University, 3-1-1 Maidashi, Higashi-ku, Fukuoka 812-8582, Japan

Table S1 Primers for qRT-PCR

Target	Forward	bp	Reverse	bp
NDUFA1	AAGGACCCAGAAGTAGGGTTTT	22	CAGTGATACCCAAAATGAGCAA	22
NDUFA9	AAATCCTTTGCTTTCGTTGGT	21	TTGTTATCCAGGGCTCAAATG	21
NDUFA10	GATCGGGGGAGGGTAAATAA	20	CAGCAGACCACTGTTTTCCA	20
NDUFB2	ACTGCTGGAGATGGTGGAGT	20	GACCCAGCACCTCTTCTGAG	20
NDUFB8	TACAACAGGAACCGTGTGGA	20	CTGGTTCTTTGGAGGGATCA	20
NDUFS7	AGTTCTCTGTGGCCCATGAC	20	GGCATCTGGTCGTAGACCTT	20
NDUFV1	AGCTTCATGAATAAGCCCTCAG	22	TAGAATTCCCCTCGGATGTAGA	22
NDUFV2	AATGTTTAGGGGCCTGTGTG	20	AGCTGGCTCACAAGAGAAGC	20
SDHA	TCGCACTGTGCATAGAGGAC	20	ATGCCTGTAGGGTGGAACTG	20
SDHB	TAAATGTGGCCCCATGGTAT	20	AGGTTGGTGTCAATCCTTCG	20
SDHC	TGAGTGCAGGGGTCTCTCTT	20	GGAATCTTCAGGCCTTTTCC	20
SDHD	GTATGCCTCTTTGCCTCTGC	20	GAGGCAACCCCATTAACTCA	20
CYC1	CCAGCTACCATGTCCCAGAT	20	TATGCCAGCTTCCGACTCTT	20
UQCRC1	TGTCTCGTGCAGACTTGACC	20	GAAGCGGCATGGAGTAAGAG	20
UQCRFS1	GGAAATTGAGCAGGAAGCTG	20	GGCAAGGGCAGTAATAACCA	20
UQCRH	TTGCTGCTCGTGTTGAATCT	20	CTCGCATTGCTCTCTCACTG	20
COX5A	GCATGCAGACGGTTAAATGA	20	AGTTCCTCCGGAGTGGAGAT	20
COX17	AGGAGAAGAAGCCGCTGAAG	20	ATTCACACAGCAGACCACCA	20
SCO1	GGGGAGCTAAAACTGACAA	20	TGGGTCAATGCTGATGAAAA	20
ATP5A1	GTGGCTCCTTGACTGCTTTG	20	ACCTGCTTCATAGCCCTGGT	20
ATP5C1	GCCAAGCTGTCATCACAAAA	20	GGACAAAGGCAGCAGTAAGC	20
ATP5D	GGAAGCTCCTCCTCAGCTTT	20	CAGGCTTCCGGGTCTTTAAT	20
ATP5G1	ACATTGACACAGCAGCCAAG	20	GCCAAGAATGGCATAGGAGA	20
ATPAF2	GAGATCAGCTCCTCCACCAG	20	TCAATCAGGCCCAAGGTTAG	20
18S rRNA	CATGGCCGTTCTTAGTTGGT	20	CGCTGAGCCAGTCAGTGTAG	20
28S rRNA	ACCGTCGTGAGACAGGTTAGTT	22	CGTTCAGTCATAATCCCACAGA	22

Received 3 October 2011/5 January 2012; accepted 27 January 2012
Published as BJ Immediate Publication 27 January 2012, doi:10.1042/BJ20111728

[1] To whom correspondence should be addressed (email uchiumi@cclm.med.kyushu-u.ac.jp).

THE JOURNAL OF BIOLOGICAL CHEMISTRY VOL. 287, NO. 5, pp. 3265–3272, January 27, 2012

Mitophagy Plays an Essential Role in Reducing Mitochondrial Production of Reactive Oxygen Species and Mutation of Mitochondrial DNA by Maintaining Mitochondrial Quantity and Quality in Yeast*[S]

Received for publication, July 7, 2011, and in revised form, November 16, 2011 Published, JBC Papers in Press, December 7, 2011, DOI 10.1074/jbc.M111.280156

Yusuke Kurihara, Tomotake Kanki[1], Yoshimasa Aoki, Yuko Hirota, Tetsu Saigusa, Takeshi Uchiumi, and Dongchon Kang

From the Department of Clinical Chemistry and Laboratory Medicine, Kyushu University Graduate School of Medical Sciences, Fukuoka 812-8582, Japan

Background: The physiological importance of mitophagy in yeast has been largely unexplored.
Results: Mitochondrial DNA deletion frequently occurs in mitophagy-deficient cells during nitrogen starvation because of overproduction of the reactive oxygen species from unregulated mitochondria.
Conclusion: Mitophagy prevents excess reactive oxygen species production and mitochondrial DNA mutation.
Significance: Our findings provide insight into mitophagy-related disorders such as Parkinson disease.

In mammalian cells, the autophagy-dependent degradation of mitochondria (mitophagy) is thought to maintain mitochondrial quality by eliminating damaged mitochondria. However, the physiological importance of mitophagy has not been clarified in yeast. Here, we investigated the physiological role of mitophagy in yeast using mitophagy-deficient *atg32*- or *atg11*-knock-out cells. When wild-type yeast cells in respiratory growth encounter nitrogen starvation, mitophagy is initiated, excess mitochondria are degraded, and reactive oxygen species (ROS) production from mitochondria is suppressed; as a result, the mitochondria escape oxidative damage. On the other hand, in nitrogen-starved mitophagy-deficient yeast, excess mitochondria are not degraded and the undegraded mitochondria spontaneously age and produce surplus ROS. The surplus ROS damage the mitochondria themselves and the damaged mitochondria produce more ROS in a vicious circle, ultimately leading to mitochondrial DNA deletion and the so-called "petite-mutant" phenotype. Cells strictly regulate mitochondrial quantity and quality because mitochondria produce both necessary energy and harmful ROS. Mitophagy contributes to this process by eliminating the mitochondria to a basal level to fulfill cellular energy requirements and preventing excess ROS production.

Autophagy is a protein degradation process that involves the formation of a double-membrane compartment, termed the autophagosome, which engulfs cytoplasmic components non-selectively and fuses with the lysosome/vacuole for degradation (1). This is important for various physiological processes such as cell survival under starvation, intracellular clearance, development, the immune response, and aging (2).

Recent studies have revealed that autophagy can degrade mitochondria selectively. This autophagic mitochondrial degradation is called mitophagy (3, 4). Recently, the mitochondrial protein Atg32, which is specifically required for mitophagy, was identified in yeast, and studies of Atg32 have revealed the molecular processes of mitochondrial selection by the autophagic machineries (5–9). In brief, when mitophagy is initiated, the mitochondrial outer-membrane protein Atg32 is recognized and bound by the cytosolic adaptor protein Atg11. Atg11 recruits the mitochondria to the pre-autophagosomal structure/phagophore assembly site where the phagophores, the initial sequestering membrane structures, are generated to uptake and degrade mitochondria (10, 11). Although this molecular mechanism is known, the physiological importance of mitophagy in yeast has been largely unexplored.

It is believed that mitophagy in mammalian cells functions in mitochondrial quality control. Loss-of-function mutations in the *PARK2* and *PARK6* genes, which encode Parkin and PINK1, respectively, cause Parkinson disease. Recent studies have linked Parkin and PINK1 to mitophagy (12–14). Cytosolically synthesized PINK1 can target and stably localize on damaged mitochondria, and mitochondrial PINK1 translocates the cytosolic E3 ubiquitin ligase Parkin to the mitochondria (15–19). Finally, the damaged mitochondria are degraded by Parkin-mediated mitophagy, although the details of this process have not been revealed. These findings imply that PINK1/Parkin-mediated mitophagy plays a very important role in the quality control of mitochondria, eliminating damaged mitochondria selectively, and that dysfunction of this mitophagic process causes Parkinson disease (12–14).

The importance of mitophagy in mammalian cells suggests that mitophagy also plays an important physiological role in

* This work was supported by Grants-in-aid for Scientific Research 23689032 (to T. K.), 22020028 (to T. K.), and 22249018 (to D. K.) from the Ministry of Education, Culture, Sports, Science and Technology of Japan, a grant from the Takeda Science Foundation (to T. K.), the Naito Foundation (to T. K.), the Mochida Memorial Foundation for Medical and Pharmaceutical Research (to T. K.), the Kowa Life Science Foundation (to T. K.), and the Kyushu University Interdisciplinary Programs in Education and Projects in Research Development (to T. K.).
[S] This article contains supplemental Figs. S1–S5.
[1] To whom correspondence should be addressed: 3-1-1 Maidashi, Higashi-ku, Fukuoka 812-8582, Japan. Tel.: 81-92-642--5752; Fax: 81-92-642-5772; E-mail: kanki@cclm.med.kyushu-u.ac.jp.

TABLE 1
Yeast strains used in this study

Strain	Genotype	Source
SEY6210	MATα *his3-Δ200 leu2–3,112 lys2–801 trp1-Δ901 ura3–52 suc2-Δ9 GAL*	29
TKYM139	SEY6210 *atg32Δ::LEU2*	This study
WHY1	SEY6210 *atg1Δ::HIS5 s.p.*	30
YTS147	SEY6210 *atg11Δ::LEU2*	8
BY4742	MATα *his3Δ1 leu2Δ0 lys2Δ0 ura3Δ0*	Open Biosystems, Huntsville, AL
BYATG1	BY4742 *atg1Δ::KAN*	Open Biosystems
BYATG11	BY4742 *atg11Δ::KAN*	Open Biosystems
BYATG32	BY4742 *atg32Δ::KAN*	Open Biosystems

yeast. Accordingly, we examined the phenotypes associated with mitophagy-deficient *atg32Δ* and *atg11Δ* cells and found that mitochondrial DNA (mtDNA)[2] deletion frequently occurs in mitophagy-deficient cells during nitrogen starvation, especially if the cells are in respiratory growth before starvation. Further analysis revealed that when wild-type cells encounter nitrogen starvation, they initiate mitophagy and quickly eliminate mitochondria that have proliferated during respiratory growth. As a result, cellular reactive oxygen species (ROS) production, which occurs mainly in mitochondria, is suppressed. On the other hand, in mitophagy-deficient cells, undegraded mitochondria produce excess ROS during nitrogen starvation. ROS damage mitochondria and damaged mitochondria produce more ROS, and finally, overproduced ROS cause mtDNA deletion. Ultimately, cells with mtDNA deletion generate small colonies even on fermentable medium, and this phenotype is called "petite" (20). From these findings, we conclude that mitophagy prevents mtDNA deletion by eliminating ROS-producing mitochondria during nitrogen starvation.

EXPERIMENTAL PROCEDURES

Strains, Culture Media, and Antibodies—The yeast strains used in this study are listed in Table 1. Yeast cells were grown in rich medium (YPD; 1% yeast extract, 2% peptone, 2% glucose), lactate medium (YPL; 1% yeast extract, 2% peptone, 2% lactate), or ethanol glycerol medium (YPEG; 1% yeast extract, 2% peptone, 3% ethanol, 3% glycerol). Nitrogen starvation experiments were performed in synthetic minimal medium lacking nitrogen (SD-N; 0.17% yeast nitrogen base without amino acids and ammonium sulfate, 2% glucose). Anti-Cox2 antibodies (Invitrogen), anti-Por1 antibodies (Invitrogen), and anti-Pgk1 antibodies (Nordic Immunological Laboratories, Eindhoven, The Netherlands) were used for immunoblotting.

Assessment of Viability by Colony Formation Assay—The cellular viability assay was performed as described previously with some modifications (21). Briefly, cells grown in YPD or YPL to mid-log phase were washed twice with water and cultured in SD-N. On the indicated days, the cells contained in 0.02 μl of SD-N were inoculated onto YPD plates. After 2 days, the number and size of the resulting colonies were measured.

Measurement of ROS—Cells were incubated in staining buffer (10 μM dihydroethidium (DHE), 100 mM HEPES, pH 7.5, 5% glucose) for 10 min at room temperature and then loaded onto a flow cytometer (BD Biosciences) to observe the oxidized DHE fluorescence. To detect protein oxidization, we used an OxyBlot™ Protein Oxidation Detection kit (Millipore, Billerica, MA) according to the manufacturer's instructions.

Southern Blotting—Cells were cultured in YPD medium to mid-log phase, and whole cell DNA was extracted by standard methods. Five milligrams of whole cell DNA was digested with BamHI (Takara, Kyoto, Japan) or ScaI (Takara), separated on a 0.8% agarose gel, and transferred onto Hybond-N$^+$ nylon membrane (GE Healthcare). The *COX1* and *COB* coding regions were amplified by PCR using primers 5′-GGTATGGCAGGAACAGCAAT-3′ and 5′-ACAGCCCTCCAAATGTCAAC-3′ for *COX1*, and 5′-ATGATTGGCCGGTTTAATTG-3′ and 5′-TATGGGAGTTCCCACAAAGC-3′ for *COB*. The PCR products were labeled with alkaline phosphatase using AlkPhos Direct Labeling reagents (GE Healthcare) and used as probes on the blots. The signals were detected with CDP-star (GE Healthcare), according to the manufacturer's instructions.

RESULTS

Mitophagy-deficient Cells Generate Small Colonies—We have previously examined cell viability during nitrogen starvation in *atg32Δ* cells, and found that both wild-type and *atg32Δ* cells grew to a similar level (7). In our previous experiment, we pre-cultured cells in a fermentable carbon source-containing medium (YPD: yeast extract, peptone, and dextrose) before nitrogen starvation. We speculated that more drastic conditions might be required to elucidate a phenotype in mitophagy-deficient cells. Here, we pre-cultured cells in a nonfermentable carbon source-containing medium (YPL: yeast extract, peptone, and lactate) in which mitochondria proliferate for respiratory growth, and then shifted the cells to nitrogen starvation medium (SD-N) and observed the cell viability according to the duration of nitrogen starvation. Contrary to our expectations, both the wild-type (SEY6210) and mitophagy-deficient *atg32Δ* and *atg11Δ* cells survived at similar levels during nitrogen starvation, whereas macroautophagy-deficient *atg1Δ* cells became almost nonviable after 12 days of nitrogen starvation (supplemental Fig. S1*A*). During this experiment, we found that mitophagy-deficient cells tended to form smaller colonies than wild-type cells when inoculated onto a YPD plate after nitrogen starvation. For example, after 5 days of nitrogen starvation, almost all the wild-type cells formed uniformly normal-sized colonies on a YPD plate, whereas *atg32Δ* and *atg11Δ* cells also formed relatively small colonies (hereafter we call the normal-sized colonies "large colonies" to distinguish them from the

[2] The abbreviations used are: mtDNA, mitochondrial DNA; DHE, dihydroethidium; ROS, reactive oxygen species; SD-N, synthetic minimal medium lacking nitrogen; YPD, yeast extract, peptone, glucose; YPEG, yeast extract, peptone, ethanol, glycerol; YPL, yeast extract, peptone, lactate.

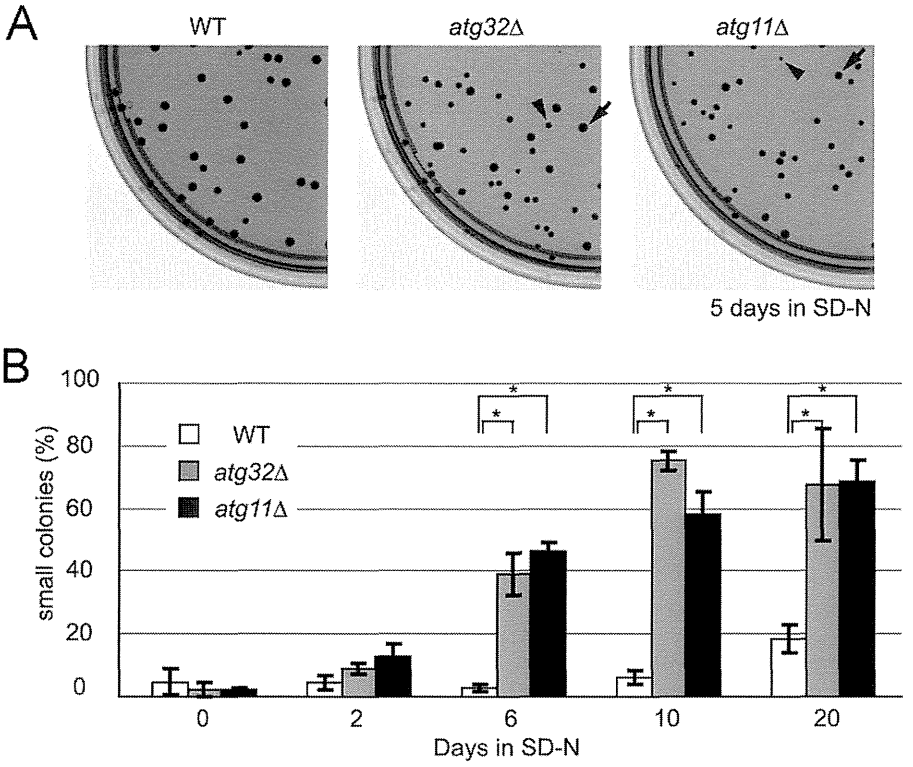

FIGURE 1. **Mitophagy-deficient cells generate small colonies after nitrogen starvation.** *A*, wild-type (*WT*), *atg32*Δ, and *atg11*Δ cells were pre-cultured in YPL to mid-log phase and then shifted to SD-N for 5 days. Cells were inoculated onto YPD plates and the size of colonies formed was observed (typical small and large colonies are indicated by *arrowheads* and *arrows*, respectively). *B*, WT, *atg32*Δ, and *atg11*Δ cells were precultured in YPL to mid-log phase and then shifted to SD-N. After the indicated number of days of nitrogen starvation, cells were inoculated onto YPD plates and the proportion of small colonies formed was observed (more than 80 colonies were measured for each experiment). The values represent the mean ± S.D. of three experiments. *, $p < 0.001$ by paired *t* test.

small colonies) (Fig. 1*A*). As a control, we cultured wild-type, *atg32*Δ, and *atg11*Δ cells without starvation for 5 days and then inoculated the cells onto YPD plates. Both wild-type and mitophagy-deficient cells barely formed small colonies (wild-type, 1.88 ± 0.62%; *atg32*Δ, 2.12 ± 1.19%; *atg11*Δ, 1.63 ± 0.50%; supplemental Fig. S1*B*). We pre-cultured wild-type, *atg32*Δ, and *atg11*Δ cells in YPL medium and then shifted them to SD-N for up to 20 days, then inoculated the cells onto YPD plates and observed the proportion of small colonies, defined as those with a diameter less than 50% of that of a typical large colony. As shown in Fig. 1*B*, the proportion of small colonies was ~40% for both *atg32*Δ and *atg11*Δ cells after 6 days of nitrogen starvation, and the proportion was further increased with a longer duration of nitrogen starvation. In contrast, in wild-type cells, the proportion of small colonies was less than 5% even after 10 days of nitrogen starvation, and it increased up to ~20% after 20 days of nitrogen starvation.

To confirm the phenotype observed above, we repeated the same experiment using a different background strain (BY4742). Surprisingly, even wild-type cells almost lost their viability after 14 days of nitrogen starvation (supplemental Fig. S2*A*). Mitophagy-deficient *atg32*Δ and *atg11*Δ cells lost their viability earlier than wild-type cells did, but the difference was not significant (supplemental Fig. S2*A*). As for SEY6210 cells, *atg32*Δ and *atg11*Δ cells of BY4742 tended to form small colonies on YPD plates after nitrogen starvation, with the frequency depending on the duration of starvation (supplemental Fig. S2, *B* and *C*). Because cells that formed small colonies generated small colonies again when they were inoculated onto new YPD plates, we speculated that inheritable damage, such as genomic DNA or mtDNA mutation, might have occurred in these cells.

mtDNA Deletion in Mitophagy-deficient Yeast Cells—We presumed that a mitochondrial defect was the most likely cause of small colony generation. To test this, we reinoculated both large and small colonies derived from wild-type, *atg32*Δ, and *atg11*Δ strains onto YPL and YPEG (yeast extract, peptone, ethanol, and glycerol) plates, on which mitochondria-dependent respiration is essential for cellular growth. Although all cells from large colonies could grow on YPL and YPEG plates, cells from small colonies could not grow on YPL or YPEG plates (Fig. 2*A*), suggesting that the latter cells have a mitochondrial defect. To examine the mitochondrial defect further, we investigated the expression levels of mitochondrial proteins in large and small colony-forming cells. Surprisingly, cells forming small colonies did not express any of the mtDNA-encoded mitochondrial inner membrane protein Cox2, whereas cells forming either large or small colonies expressed the nuclear genome-encoded mitochondrial outer membrane protein Por1 to a similar extent (Fig. 2*B*). This finding suggested that there was a defect in intramitochondrial transcription or translation, or the mtDNA itself in the cells that formed small colonies. We then examined the mtDNA by Southern blotting. Whole cell DNA prepared from cells forming either small or large colonies was digested with BamHI or ScaI, Southern blotted, and probed with mtDNA-derived probes: the *COX1* or *COB* coding regions. For all large colony-forming cells, we detected bands of

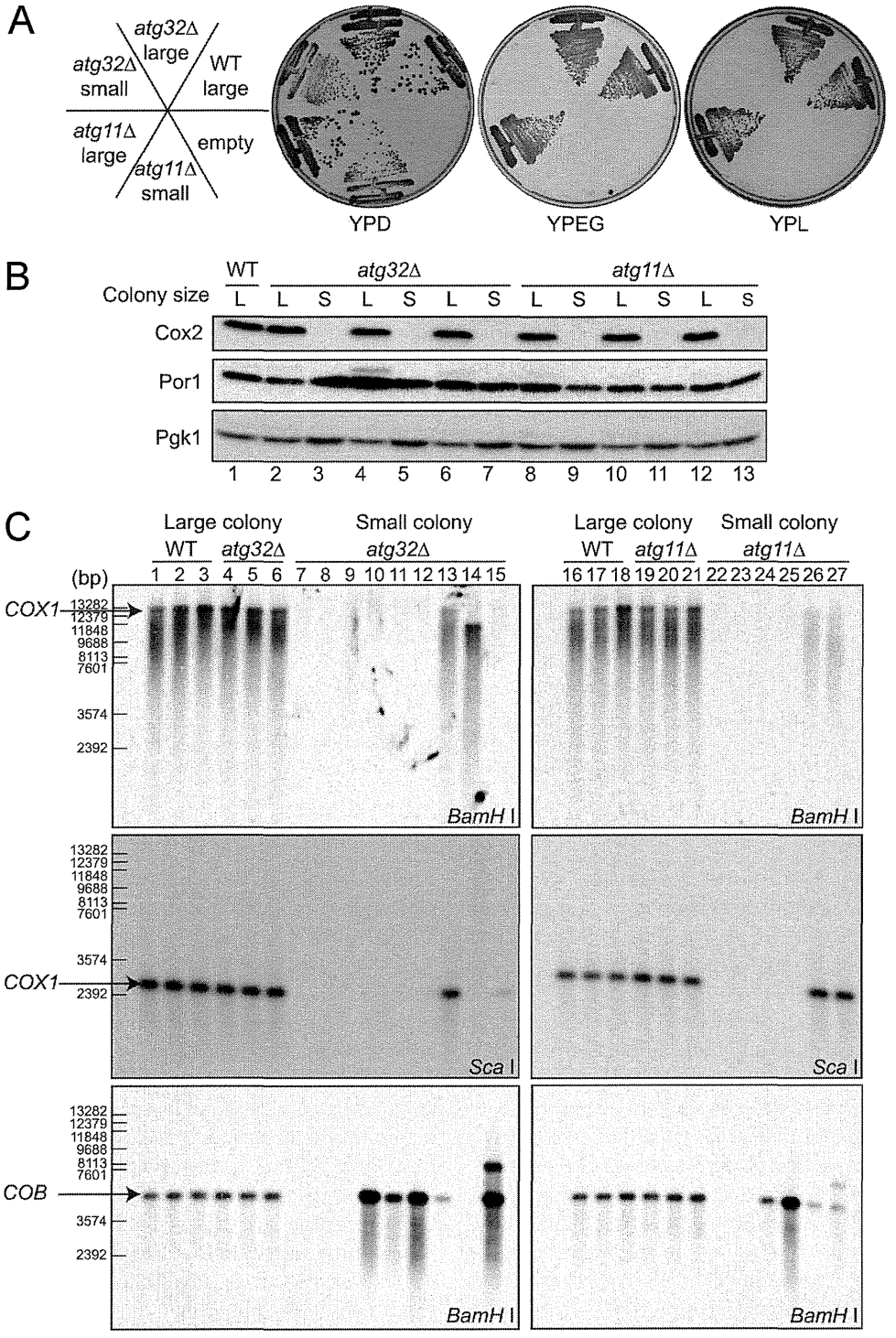

FIGURE 2. **Mitochondrial DNA deletion occurs in mitophagy-deficient strains during nitrogen starvation.** *A*, large and small colonies formed after 10 days of starvation were inoculated onto YPD, YPL, and YPEG plates and grown for 2–3 days at 30 °C. *atg32Δ* and *atg11Δ* small colony-derived cells only were unable to grow on YPL or YPEG. *B*, large and small colonies formed after 6 or 10 days starvation were cultured in YPD to mid-log phase (*lanes 1–5* and *8–11*, 6 days in SD-N; *lanes 6, 7, 12*, and *13*, 10 days in SD-N). Cell lysates were immunoblotted with anti-Cox2, anti-Por1, and anti-Pgk1 (loading control) antibodies. *atg32Δ* and *atg11Δ* small colony-derived cells only did not produce the mitochondrially encoded protein Cox2. *C*, large and small colonies formed after 5 or 6 days starvation were cultured in YPD to mid-log phase. Whole cell DNA was digested by BamHI or ScaI and analyzed by Southern blotting with *COX1* and *COB* mtDNA probes. The *atg32Δ* and *atg11Δ* small colonies showed absent or aberrant *COX1* and/or *COB* bands. *WT*, wild-type.

the expected size for both the *COX1* and *COB* probes (Fig. 2*C*, *lanes 1–6* and *16–21*). On the other hand, for small colony-forming cells, *atg32Δ* or *atg11Δ*, we identified several patterns of results, suggesting that mtDNA deletion had occurred in these cells. In some cells, we could not detect any bands for the *COX1* or the *COB* probe (Fig. 2*C*, *lanes 7–9*, *22*, and *23*), suggesting that both *COX1*- and *COB*-encoding mtDNA regions were deleted, or the whole mtDNA genome was lost in these cells. In other cells, we could not detect any bands using the *COX1* probe, whereas the *COB* probe generated a band of the

expected size (Fig. 2*C*, *lanes 10–12*, *24*, and *25*), suggesting that at least the *COX1* region of the mtDNA genome was deleted in these cells. In addition, there were several atypical cases. In the cells shown in Fig. 2*C*, *lane 14*, we observed a smaller than expected band for the *COX1* probe on BamHI-digested DNA and no bands on ScaI-digested DNA; similarly we observed no bands for the *COB* probe on BamHI-digested DNA. In the cells shown in Fig. 2*C*, *lanes 15* and *27*, we observed a larger than expected band for the *COB* probe in addition to the expected size band. Finally, in the cells shown in Fig. 2*C*, *lanes 13* and *26*, we observed the expected size bands for both the *COX1* and *COB* probes when DNA was digested with BamHI, but the signals were very weak compared with those of the other samples, even though we used the same amount of DNA for each (supplemental Fig. S3*A*). These findings suggest that mtDNA deletion frequently occurs in mitophagy-deficient cells during nitrogen starvation. Next, we observed mtDNA in wild-type cells after 20 days starvation. All large colony-forming cells expressed Cox2 protein and had intact mtDNA, whereas small colony-forming cells, which comprised fewer than 20% of all colonies, did not express the Cox2 protein and had deleted mtDNA (supplemental Fig. S3, *B* and *C*). From these findings, we concluded that mtDNA deletion occurs to some degree during starvation even in wild-type cells; however, it is augmented in mitophagy-deficient cells.

Reactive Oxygen Species Cause mtDNA Deletion—We hypothesized that, in mitophagy-deficient cells during nitrogen starvation, ROS would be overproduced, and that excess ROS would cause mtDNA deletion. To investigate this, we observed cellular ROS during nitrogen starvation by staining cells with the superoxide indicator DHE, detecting oxidized DHE fluorescence by flow cytometry. Cellular ROS production was the same in wild-type, *atg32*Δ, and *atg11*Δ cells before nitrogen starvation (Fig. 3*A*, 0 days). As we expected, cellular ROS production gradually increased in *atg32*Δ and *atg11*Δ cells compared with wild-type cells, depending on the duration of nitrogen starvation (Fig. 3*A* and supplemental Fig. S4, *A* and *B*). We further examined cellular ROS production by observing protein oxidation in mitophagy-deficient cells during nitrogen starvation using an OxyBlot protein oxidation detection assay. Consistent with flow cytometry results, the levels of oxidized protein increased dramatically in *atg32*Δ and *atg11*Δ cells after nitrogen starvation, compared with wild-type cells (Fig. 3*B*).

If the overproduction of ROS in mitophagy-deficient cells was the direct cause of mtDNA damage and small colony formation, elimination of the cellular ROS may rescue the phenotype. To examine this possibility, we cultured cells with the ROS scavenger *N*-acetylcysteine and observed the size of colonies generated after nitrogen starvation. As shown in Fig. 3*C* and supplemental Fig. S5, addition of *N*-acetylcysteine dramatically decreased the proportion of small colonies after nitrogen starvation in mitophagy-deficient *atg32*Δ and *atg11*Δ cells, whereas it showed no effect in wild-type cells. From these findings, we confirmed that ROS, which are overproduced in mitophagy-deficient cells, damaged the mtDNA and caused mtDNA deletion during nitrogen starvation, causing the cells to generate small colonies on YPD plates.

Mitochondria are the major source of cellular ROS. It is highly possible that mitochondria that are not degraded by mitophagy are the source of the excess ROS in mitophagy-deficient cells. Thus, we investigated the cellular number of mitochondria using Por1 and Cox2 as mitochondrial markers. In wild-type cells, the Por1 signal quickly decreased and the Cox2 signal gradually decreased as a result of mitophagy upon nitrogen starvation, whereas in mitophagy-deficient *atg32*Δ and *atg11*Δ cells, both Por1 and Cox2 expression was barely affected by nitrogen starvation (Fig. 3*D*). This finding is consistent with our hypothesis regarding cellular ROS production: in wild-type cells, ROS production slightly decreased following the degradation of mitochondria during nitrogen starvation (supplemental Fig. S4*B*), whereas in *atg32*Δ cells, ROS production gradually increased during nitrogen starvation (supplemental Fig. S4*B*), presumably because the undegraded mitochondria became old and damaged and produced more ROS. We concluded that wild-type cells quickly degrade excess mitochondria by mitophagy during nitrogen starvation, preventing overproduction of ROS and subsequent mtDNA mutation, whereas in mitophagy-deficient cells that cannot degrade excess mitochondria, ROS produced from undegraded mitochondria cause mtDNA mutation during nitrogen starvation.

In the studies described above, we pre-cultured cells in YPL to proliferate the mitochondria before shifting to the nitrogen-starvation state. If the cells were pre-cultured in YPD, the small colony phenotype might be inhibited in mitophagy-deficient cells during nitrogen starvation, because the number of ROS producing mitochondria is smaller when cells are cultured in YPD compared with in YPL. To test this, we pre-cultured *atg32*Δ cells in either YPD or YPL, and observed the proportion of small colonies formed on YPD plates after nitrogen starvation. As expected, the proportion of small colonies was dramatically decreased in *atg32*Δ cells after nitrogen starvation when the cells were precultured in YPD compared with those precultured in YPL (22 and 39% at 6 days, 35 and 75% at 10 days of starvation, when precultured in YPD and YPL, respectively; Fig. 3*E*). This supports our notion that the ROS produced by undegraded mitochondria during nitrogen starvation cause mtDNA mutation in mitophagy-deficient cells.

DISCUSSION

Although the presence of mitochondria in lysosomes or vacuoles was first reported in 1957 in mammalian cells (22) and in 1992 in yeast (23), the physiological relevance of mitochondrial degradation by autophagy has been unclear. Very recently, in mammalian cells, several studies have suggested that PINK1/parkin-dependent mitophagy selectively degrades depolarized mitochondria (12, 18, 19), implying that mitophagy contributes to mitochondrial quality control. On the other hand, very little is known about the physiological importance of mitophagy in yeast. When we identified the mitophagy-specific gene *ATG32* in yeast, we tried to identify the physiological role of mitophagy using *atg32*Δ cells; we could not, however, identify any phenotypes associated with these cells (7). In this study, we have now identified the physiological relevance of mitophagy in yeast. When yeast cells in respiratory growth encounter nitrogen starvation, the cells initiate mitophagy, degrade excess mitochon-

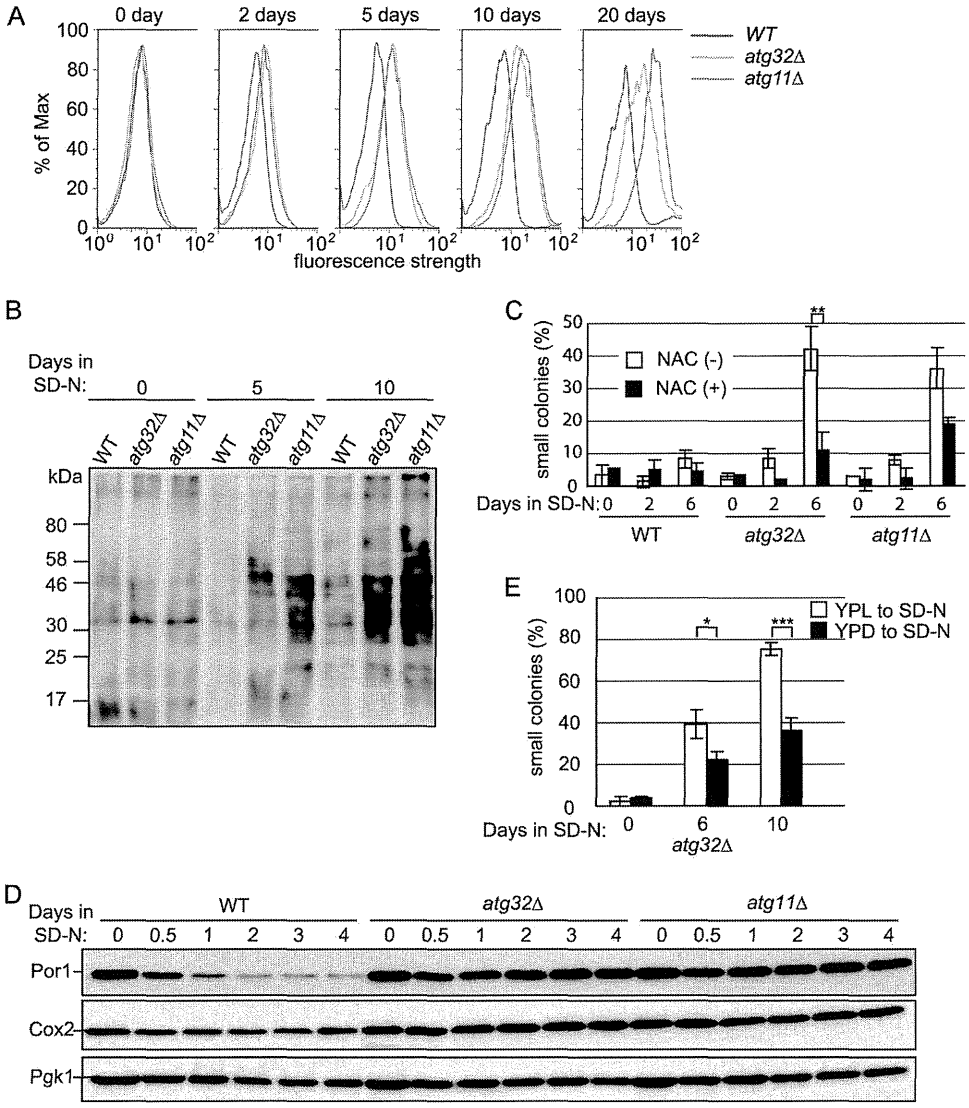

FIGURE 3. **ROS in mitophagy-deficient cells cause mtDNA deletion during nitrogen starvation.** *A,* wild-type (*WT*), *atg32*Δ, and *atg11*Δ cells were precultured in YPL to mid-log phase and then shifted to SD-N. After the indicated number of days of nitrogen starvation, cells were incubated with the superoxide indicator DHE, and oxidized DHE fluorescence was observed using flow cytometry. *B,* wild-type, *atg32*Δ, and *atg11*Δ cells were precultured in YPL to mid-log phase and then shifted to SD-N. After the indicated number of days of nitrogen starvation, oxidized proteins were observed by OxyBlot assay. *C,* WT, *atg32*Δ, and *atg11*Δ cells were precultured in YPL to mid-log phase and then shifted to SD-N containing 1 mM of the ROS scavenger *N*-acetylcysteine (*NAC*) or dimethyl sulfoxide (control). After the indicated number of days of nitrogen starvation, cells were inoculated onto YPD plates and the proportion of small colonies formed on YPD plates was calculated (more than 80 colonies were measured for each experiment). The values represent the mean ± S.D. of three experiments. *D,* WT, *atg32*Δ, and *atg11*Δ cells were precultured in YPL to mid-log phase and then shifted to SD-N. Cells were collected after the indicated number of days of nitrogen starvation and cell lysates were immunoblotted with anti-Cox2, anti-Por1, and anti-Pgk1 (loading control) antibodies. *E,* WT and *atg32*Δ cells were precultured in YPD or YPL to mid-log phase and then shifted to SD-N. After the indicated number of days of nitrogen starvation, cells were inoculated onto YPD plates and the proportion of small colonies formed was calculated (more than 80 colonies were measured for each experiment). The values represent the mean ± S.D. of three experiments. ***, $p < 0.001$; **, $p < 0.005$; *, $p < 0.01$ by paired *t* test.

dria, and suppress ROS production from mitochondria, and as a result, the cells escape the severe oxidative damage that causes mtDNA deletion. This process is very important for yeast in nature, because the cells frequently shift their metabolism between fermentation and respiration and are always at risk of starvation.

Our current scheme based on this study is summarized in Fig. 4. When yeast cells grow in glucose-rich conditions, such as on the surface of grapes, they preferentially ferment glucose and release ethanol. When cells absorb glucose, they switch their metabolism from fermentation to respiration, the aerobic usage of ethanol. This conversion (called the diauxic shift) is frequently observed in nature. During the diauxic shift, mitochondria proliferate to increase cellular respiration. If the cells then encounter starvation stress, for example, if the nutrients are washed away by rain, mitophagy is initiated and the cells minimize the number of mitochondria to a basal level to fulfill cellular energy requirements, thus suppressing the production of unwanted ROS and mitochondrial damage.

It has been recently reported that bulk autophagy-deficient cells accumulate high levels of ROS and that these ROS cause the loss of mtDNA during nitrogen starvation (24). Although these phenotypes of bulk autophagy-deficient cells are similar to those of mitophagy-deficient cells, the process of ROS accumulation is totally different. In bulk autophagy-deficient cells, cellular ROS accumulate during nitrogen starvation because

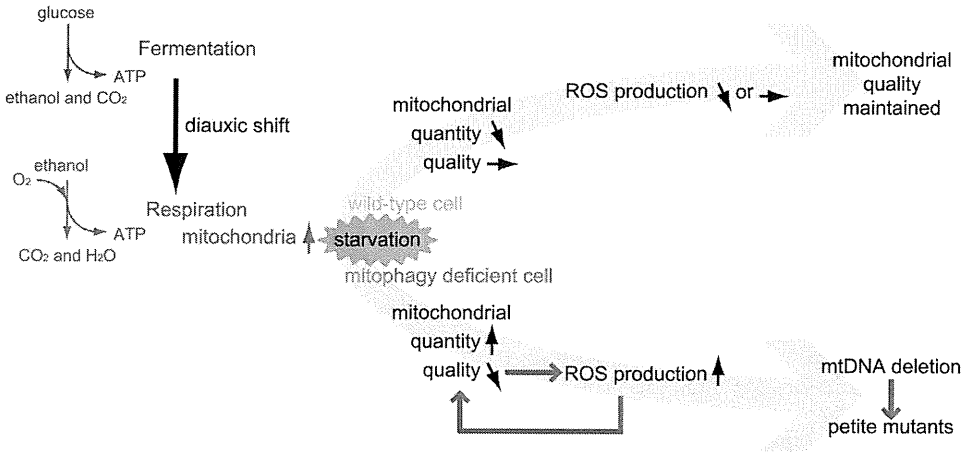

FIGURE 4. **Summary of the importance of mitophagy in yeast.** When yeast cells encounter starvation stress in respiratory growth, wild-type cells initiate mitophagy, degrade excess mitochondria, and suppress the production of ROS from mitochondria; as a result, the mitochondria escape oxidative damage. In mitophagy-deficient cells, the mitochondria suffer oxidative damage and produce more ROS that ultimately cause mtDNA mutation.

the cellular amino acid pool is reduced and the expression of mitochondrial respiratory proteins and the ROS scavenger proteins is suppressed (24). Moreover, the level of ROS accumulated in bulk autophagy-deficient cells during nitrogen starvation was much higher than that in mitophagy-deficient or wild-type cells (data not shown).

It is believed that mitophagy in mammalian cells functions in mitochondrial quality control. There are, however, limited experimental data showing the physiological importance of mitophagy for quality control of mitochondria in mammalian cells, except for PINK1/Parkin-dependent mitophagy. One reason for this is that mitophagy-specific genes such as *ATG32* in yeast have not been identified in mammals. Furthermore, although it is clear that PINK1/Parkin-dependent mitophagy, especially when Parkin is overexpressed, eliminates dysfunctional mitochondria in cultured cells, the physiological phenotypes of mitophagy deficient (Parkin knock-out mice or Parkin knockdown cells, for example) have been poorly characterized (25–28). In this article, we clearly demonstrate the physiological importance of mitophagy to maintain mitochondrial quality in yeast. Because mitophagy is conserved from yeast to mammals, the fundamental processes and roles of mitophagy are expected to be similar between yeast and mammals, although they may be highly diverse among mammalian cells. Further studies are required to elucidate the details of these processes in mammals, and to assess their impact on human diseases such as Parkinson disease.

Acknowledgment—We thank Daniel J. Klionsky (University of Michigan) for providing the yeast strains and plasmids.

REFERENCES

1. Nakatogawa, H., Suzuki, K., Kamada, Y., and Ohsumi, Y. (2009) Dynamics and diversity in autophagy mechanisms. Lessons from yeast. *Nat. Rev. Mol. Cell Biol.* **10,** 458–467
2. Mizushima, N., Levine, B., Cuervo, A. M., and Klionsky, D. J. (2008) Autophagy fights disease through cellular self-digestion. *Nature* **451,** 1069–1075
3. Lemasters, J. J. (2005) Selective mitochondrial autophagy, or mitophagy, as a targeted defense against oxidative stress, mitochondrial dysfunction, and aging. *Rejuvenation Res.* **8,** 3–5
4. Priault, M., Salin, B., Schaeffer, J., Vallette, F. M., di Rago, J. P., and Martinou, J. C. (2005) Impairing the bioenergetic status and the biogenesis of mitochondria triggers mitophagy in yeast. *Cell Death Differ.* **12,** 1613–1621
5. Kanki, T., Wang, K., Baba, M., Bartholomew, C. R., Lynch-Day, M. A., Du, Z., Geng, J., Mao, K., Yang, Z., Yen, W. L., and Klionsky, D. J. (2009) A genomic screen for yeast mutants defective in selective mitochondria autophagy. *Mol. Biol. Cell* **20,** 4730–4738
6. Okamoto, K., Kondo-Okamoto, N., and Ohsumi, Y. (2009) Mitochondria-anchored receptor Atg32 mediates degradation of mitochondria via selective autophagy. *Dev. Cell* **17,** 87–97
7. Kanki, T., Wang, K., Cao, Y., Baba, M., and Klionsky, D. J. (2009) Atg32 is a mitochondrial protein that confers selectivity during mitophagy. *Dev. Cell* **17,** 98–109
8. Kanki, T., and Klionsky, D. J. (2008) Mitophagy in yeast occurs through a selective mechanism. *J. Biol. Chem.* **283,** 32386–32393
9. Aoki, Y., Kanki, T., Hirota, Y., Kurihara, Y., Saigusa, T., Uchiumi, T., and Kang, D. (2011) Phosphorylation of serine 114 on Atg32 mediates mitophagy. *Mol. Biol. Cell* **22,** 3206–3217
10. Kanki, T., Klionsky, D. J., and Okamoto, K. (2011) *Antioxid Redox Signal.* **14,** 1989–2001
11. Kanki, T., and Klionsky, D. J. (2010) The molecular mechanism of mitochondria autophagy in yeast. *Mol. Microbiol.* **75,** 795–800
12. Youle, R. J., and Narendra, D. P. (2011) Mechanisms of mitophagy. *Nat. Rev. Mol. Cell Biol.* **12,** 9–14
13. Deas, E., Wood, N. W., and Plun-Favreau, H. (2011) Mitophagy and Parkinson disease. The PINK1-parkin link. *Biochim. Biophys. Acta* **1813,** 623–633
14. Vives-Bauza, C., and Przedborski, S. (2011) Mitophagy, the latest problem for Parkinson disease. *Trends Mol. Med.* **17,** 158–165
15. Vives-Bauza, C., Zhou, C., Huang, Y., Cui, M., de Vries, R. L., Kim, J., May, J., Tocilescu, M. A., Liu, W., Ko, H. S., Magrané, J., Moore, D. J., Dawson, V. L., Grailhe, R., Dawson, T. M., Li, C., Tieu, K., and Przedborski, S. (2010) PINK1-dependent recruitment of Parkin to mitochondria in mitophagy. *Proc. Natl. Acad. Sci. U.S.A.* **107,** 378–383
16. Geisler, S., Holmström, K. M., Skujat, D., Fiesel, F. C., Rothfuss, O. C., Kahle, P. J., and Springer, W. (2010) PINK1/Parkin-mediated mitophagy is dependent on VDAC1 and p62/SQSTM1. *Nat. Cell Biol.* **12,** 119–131
17. Ziviani, E., Tao, R. N., and Whitworth, A. J. (2010) *Drosophila* parkin requires PINK1 for mitochondrial translocation and ubiquitinates mitofusin. *Proc. Natl. Acad. Sci. U.S.A.* **107,** 5018–5023
18. Narendra, D. P., Jin, S. M., Tanaka, A., Suen, D. F., Gautier, C. A., Shen, J., Cookson, M. R., and Youle, R. J. (2010) PINK1 is selectively stabilized on impaired mitochondria to activate Parkin. *PLoS Biol.* **8,** e1000298
19. Narendra, D., Tanaka, A., Suen, D. F., and Youle, R. J. (2008) Parkin is recruited selectively to impaired mitochondria and promotes their autophagy. *J. Cell Biol.* **183,** 795–803

20. Ferguson, L. R., and von Borstel, R. C. (1992) Induction of the cytoplasmic "petite" mutation by chemical and physical agents in *Saccharomyces cerevisiae*. *Mutat. Res.* **265,** 103–148
21. Noda, T. (2008) Viability assays to monitor yeast autophagy. *Methods Enzymol.* **451,** 27–32
22. Clark, S. L., Jr. (1957) Cellular differentiation in the kidneys of newborn mice studies with the electron microscope. *J. Biophys. Biochem. Cytol.* **3,** 349–362
23. Takeshige, K., Baba, M., Tsuboi, S., Noda, T., and Ohsumi, Y. (1992) Autophagy in yeast demonstrated with proteinase-deficient mutants and conditions for its induction. *J. Cell Biol.* **119,** 301–311
24. Suzuki, S. W., Onodera, J., and Ohsumi, Y. (2011) Starvation induced cell death in autophagy-defective yeast mutants is caused by mitochondria dysfunction. *PLoS One* **6,** e17412
25. Perez, F. A., and Palmiter, R. D. (2005) Parkin-deficient mice are not a robust model of parkinsonism. *Proc. Natl. Acad. Sci. U.S.A.* **102,** 2174–2179
26. Goldberg, M. S., Fleming, S. M., Palacino, J. J., Cepeda, C., Lam, H. A., Bhatnagar, A., Meloni, E. G., Wu, N., Ackerson, L. C., Klapstein, G. J., Gajendiran, M., Roth, B. L., Chesselet, M. F., Maidment, N. T., Levine, M. S., and Shen, J. (2003) Parkin-deficient mice exhibit nigrostriatal deficits but not loss of dopaminergic neurons. *J. Biol. Chem.* **278,** 43628–43635
27. Itier, J. M., Ibanez, P., Mena, M. A., Abbas, N., Cohen-Salmon, C., Bohme, G. A., Laville, M., Pratt, J., Corti, O., Pradier, L., Ret, G., Joubert, C., Periquet, M., Araujo, F., Negroni, J., Casarejos, M. J., Canals, S., Solano, R., Serrano, A., Gallego, E., Sanchez, M., Denefle, P., Benavides, J., Tremp, G., Rooney, T. A., Brice, A., and Garcia de Yebenes, J. (2003) Parkin gene inactivation alters behavior and dopamine neurotransmission in the mouse. *Hum. Mol. Genet.* **12,** 2277–2291
28. Von Coelln, R., Thomas, B., Savitt, J. M., Lim, K. L., Sasaki, M., Hess, E. J., Dawson, V. L., and Dawson, T. M. (2004) Loss of locus coeruleus neurons and reduced startle in parkin null mice. *Proc. Natl. Acad. Sci. U.S.A.* **101,** 10744–10749
29. Robinson, J. S., Klionsky, D. J., Banta, L. M., and Emr, S. D. (1988) Protein sorting in *Saccharomyces cerevisiae*. Isolation of mutants defective in the delivery and processing of multiple vacuolar hydrolases. *Mol. Cell. Biol.* **8,** 4936–4948
30. Shintani, T., Huang, W. P., Stromhaug, P. E., and Klionsky, D. J. (2002) Mechanism of cargo selection in the cytoplasm to vacuole targeting pathway. *Dev. Cell* **3,** 825–837

nature genetics

Genome-wide association study identifies eight new susceptibility loci for atopic dermatitis in the Japanese population

Tomomitsu Hirota[1], Atsushi Takahashi[2], Michiaki Kubo[3], Tatsuhiko Tsunoda[4], Kaori Tomita[5], Masafumi Sakashita[5], Takechiyo Yamada[5], Shigeharu Fujieda[5], Shota Tanaka[1,6], Satoru Doi[7], Akihiko Miyatake[8], Tadao Enomoto[9], Chiharu Nishiyama[10], Nobuhiro Nakano[10], Keiko Maeda[10], Ko Okumura[10], Hideoki Ogawa[10], Shigaku Ikeda[11], Emiko Noguchi[12,13], Tohru Sakamoto[14], Nobuyuki Hizawa[14], Koji Ebe[15], Hidehisa Saeki[16], Takashi Sasaki[17], Tamotsu Ebihara[17], Masayuki Amagai[17], Satoshi Takeuchi[18], Masutaka Furue[18], Yusuke Nakamura[19] & Mayumi Tamari[1]

Atopic dermatitis is a common inflammatory skin disease caused by interaction of genetic and environmental factors. On the basis of data from a genome-wide association study (GWAS) and a validation study comprising a total of 3,328 subjects with atopic dermatitis and 14,992 controls in the Japanese population, we report here 8 new susceptibility loci: *IL1RL1-IL18R1-IL18RAP* ($P_{combined} = 8.36 \times 10^{-18}$), the major histocompatibility complex (MHC) region ($P = 8.38 \times 10^{-20}$), *OR10A3-NLRP10* ($P = 1.54 \times 10^{-22}$), *GLB1* ($P = 2.77 \times 10^{-16}$), *CCDC80* ($P = 1.56 \times 10^{-19}$), *CARD11* ($P = 7.83 \times 10^{-9}$), *ZNF365* ($P = 5.85 \times 10^{-20}$) and *CYP24A1-PFDN4* ($P = 1.65 \times 10^{-8}$). We also replicated the associations of the *FLG*, *C11orf30*, *TMEM232-SLC25A46*, *TNFRSF6B-ZGPAT*, *OVOL1*, *ACTL9* and *KIF3A-IL13* loci that were previously reported in GWAS of European and Chinese individuals and a meta-analysis of GWAS for atopic dermatitis. These findings advance the understanding of the genetic basis of atopic dermatitis.

Atopic dermatitis is a chronic, relapsing skin disorder involving disturbed skin barrier functions, cutaneous inflammatory hypersensitivity and defects in antimicrobial immune defense with a strong genetic basis[1,2]. It is well established that common loss-of-function variants in *FLG* (encoding filaggrin) are a major predisposing factor for atopic dermatitis[3,4]. Association studies in populations of diverse ancestry, meta-analyses of studies and GWAS have shown that mutation in *FLG* is strongly associated with atopic dermatitis[4–7]. Apart from *FLG*, recent GWAS of European and Chinese populations for atopic dermatitis and a meta-analysis of GWAS have reported six susceptibility loci at a genome-wide level of significance—*C11orf30*, *TMEM232-SLC25A46*, *TNFRSF6B-ZGPAT*, *OVOL1*, *ACTL9* and *KIF3A-IL13*[5–7]. To gain a better understanding of the contribution of complex genetic effects to the pathogenesis of atopic dermatitis, it is important to identify additional susceptibility loci and validate the association of previously reported loci in different ancestry groups.

We performed a GWAS in the Japanese population with 1,472 individuals with atopic dermatitis (cases) and 7,971 controls using Illumina Human OmniExpress BeadChips (**Supplementary Table 1**). We subjected genotype data from a total of 606,164 SNPs to statistical analysis after principal-component analysis (PCA) and quality control filtering, and we generated a quantile-quantile plot using the Cochran-Armitage test (**Supplementary Fig. 1a–c**). The genomic inflation factor (λ_{GC}) was 1.03, indicating that there was a low possibility of false positive associations resulting from population stratification. The Manhattan plot showed that a total of 36 SNPs within 3 chromosomal regions at 2q12, 6p21.3 and 11p15.4 had associations that reached the genome-wide significance threshold of $P < 5 \times 10^{-8}$ (**Fig. 1**).

GWAS of European and Chinese populations and a meta-analysis of GWAS have reported seven susceptibly regions for atopic

[1]Laboratory for Respiratory Diseases, Center for Genomic Medicine, RIKEN, Yokohama, Japan. [2]Laboratory for Statistical Analysis, Center for Genomic Medicine, RIKEN, Minato-ku, Japan. [3]Laboratory for Genotyping Development, Center for Genomic Medicine, RIKEN, Yokohama, Japan. [4]Laboratory for Medical Informatics, Center for Genomic Medicine, RIKEN, Yokohama, Japan. [5]Department of Otorhinolaryngology, Fukui Medical University, Matsuoka, Japan. [6]Department of Otolaryngology–Head and Neck Surgery, University of Yamanashi, Faculty of Medicine, Chuo, Japan. [7]Osaka Prefectural Medical Center for Respiratory and Allergic Diseases, Habikino, Japan. [8]Miyatake Asthma Clinic, Osaka, Japan. [9]Nonprofit Organization (NPO) Japan Health Promotion Supporting Network, Wakayama, Japan. [10]Atopy Research Center, Juntendo University School of Medicine, Bunkyo-ku, Japan. [11]Department of Dermatology, Juntendo University School of Medicine, Bunkyo-ku, Japan. [12]Department of Medical Genetics, Majors of Medical Sciences, Graduate School of Comprehensive Human Sciences, University of Tsukuba, Tsukuba, Japan. [13]Japan Science and Technology Agency, Core Research for Evolutional Science and Technology (CREST), Saitama, Japan. [14]Division of Respiratory Medicine, Institute of Clinical Medicine, University of Tsukuba, Tsukuba, Japan. [15]Department of Dermatology, Takao Hospital, Kyoto, Japan. [16]Department of Dermatology, Jikei University School of Medicine, Minato-ku, Japan. [17]Department of Dermatology, Keio University School of Medicine, Shinjuku-ku, Japan. [18]Department of Dermatology, Graduate School of Medical Sciences, Kyushu University, Fukuoka, Japan. [19]Laboratory of Molecular Medicine, The Institute of Medical Science, The University of Tokyo, Minato-ku, Japan. Correspondence should be addressed to M.T. (tamari@src.riken.jp).

Received 27 April; accepted 11 September; published online 7 October 2012; doi:10.1038/ng.2438

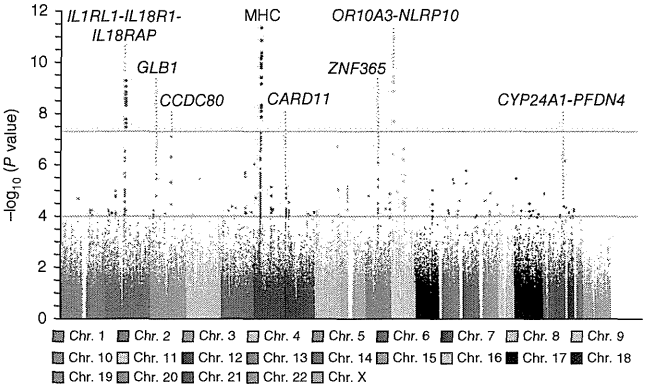

Figure 1 Manhattan plot showing the $-\log_{10} P$ values of 606,164 SNPs in the GWAS for 1,472 Japanese atopic dermatitis cases and 7,971 controls plotted against their respective positions on autosomes and the X chromosome. The red line shows the genome-wide significance threshold for this study ($P = 5 \times 10^{-8}$). The blue line shows the threshold ($P = 1 \times 10^{-4}$) for selecting SNPs for the validation study. Signals in the *IL1RL1-IL18R1-IL18RAP* (2q12), *GLB1* (3p21.33), *CCDC80* (3q13.2), MHC (6p21.3), *CARD11* (7p22), *ZNF365* (10q21.2), *OR10A3-NLRP10* (11p15.4) and *CYP24A1-PFDN4* (20q13) regions are indicated.

dermatitis[5–7]. We examined the previously reported regions in our GWAS and observed associations with atopic dermatitis for the SNPs in all of these regions (**Supplementary Fig. 2a–g** and **Supplementary Table 2**). Notably, the two regions identified in the previous GWAS of Chinese individuals had either the same SNP as the top signal in our study (20q13.3) or a SNP in strong linkage disequilibrium (LD) with the top SNP in the previous study (5q22.1); in contrast, for four of the five regions determined to be associated in Europeans, the top SNP in this study was in low LD with the previously reported best SNP.

To test for replication of the associations at the three loci suggested by the GWAS (2q12, 6p21.3 and 11p15.4) and to identify additional susceptibility loci for atopic dermatitis, we genotyped SNPs in a validation set consisting of a total of 1,856 individuals with atopic dermatitis and 7,021 controls (**Supplementary Table 1**). We first genotyped a total of ten tag SNPs ($r^2 < 0.80$) at the three loci and confirmed significant associations (**Supplementary Table 3**). We further investigated SNPs that showed P values of $<1 \times 10^{-4}$ in our GWAS and genotyped 87 tag SNPs ($r^2 < 0.80$) other than the previously reported loci and the three loci newly reported here. After Bonferroni correction with $P < 5.75 \times 10^{-4}$ (0.05/87), a total of 11 SNPs were found to be significantly associated with atopic dermatitis (**Supplementary Table 3**). We combined the data from the GWAS and

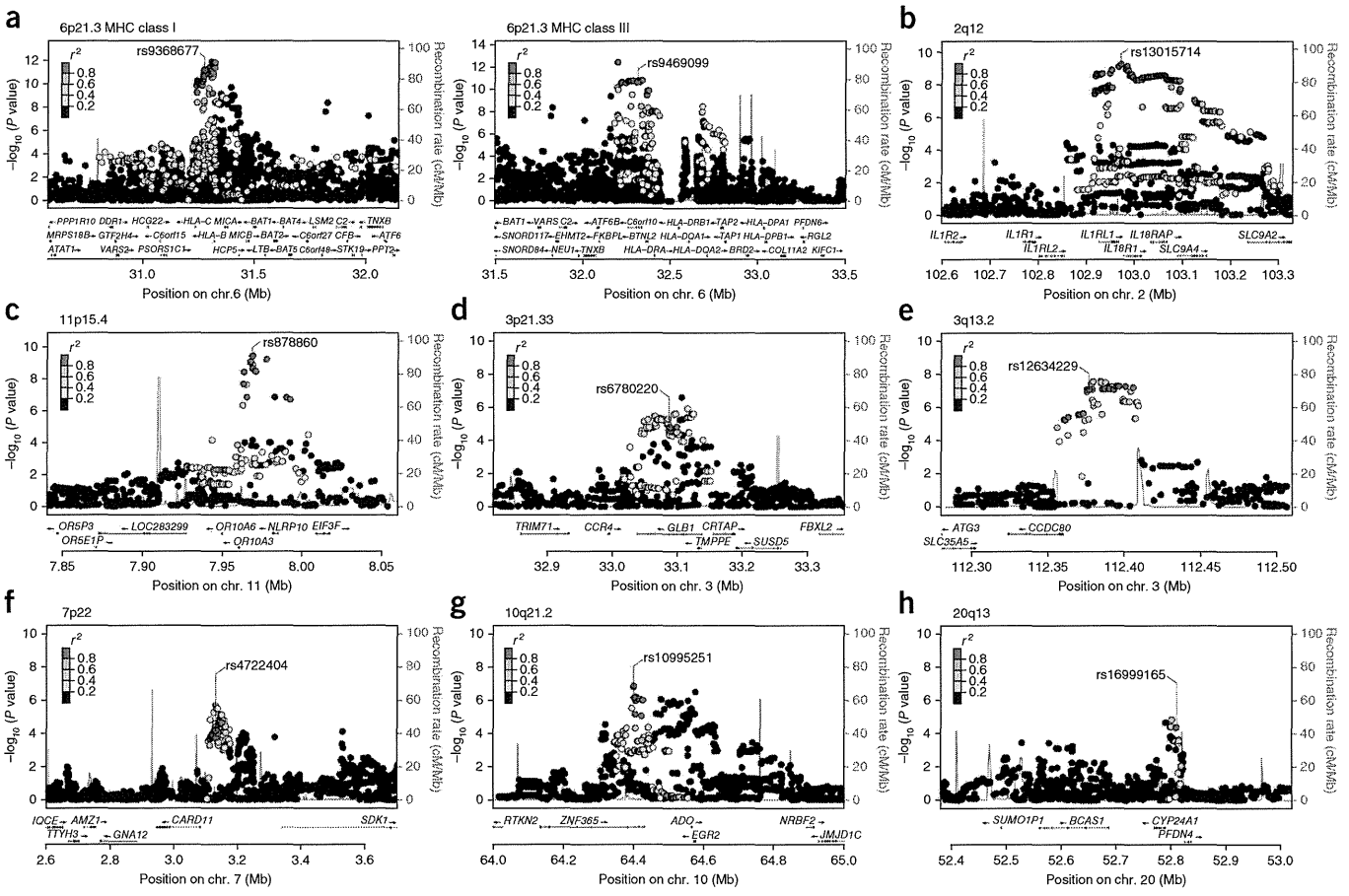

Figure 2 Regional plots of association results within eight newly identified susceptibility regions for atopic dermatitis. (**a**–**h**) Plots show the association results of both genotyped and imputed SNPs in the GWAS samples and the recombination rates within the susceptibility loci. For each plot, the $-\log_{10}$ P values (left y axis) of SNPs are shown according to their chromosomal positions (x axis). The genetic recombination rates are shown by the blue lines, and arrows indicate the locations of genes. The top genotyped SNP (labeled by rs number) is represented as a purple circle, and its LD (r^2) with the remaining SNPs is indicated by color. (**a**) MHC class I (left) and III (right) regions at 6p21.3. (**b**) 2q12. (**c**) 11p15.4. (**d**) 3p21.33. (**e**) 3q13.2. (**f**) 7p22. (**g**) 10q21.2. (**h**) 20q13.

Table 1 Summary of association results from the GWAS and validation study

SNP ID	Genes in or near regions of association	Chromosome (bp)	Allele (risk allele)	Stage	RAF Case	RAF Control	$P^{a,b}$	OR[b,c]	95% CI[b,c]	P_{het}[d]
rs13015714	*IL1RL1-IL18R1-IL18RAP*	2q12 (102971865)	T/G (G)	GWAS	0.473	0.412	5.17×10^{-10}	1.28	1.19–1.39	
				Validation	0.466	0.412	2.20×10^{-9}	1.25	1.16–1.34	
				Combined	0.470	0.412	8.36×10^{-18}	1.27	1.20–1.34	0.637
rs176095	*GPSM3* (MHC region)	6p21.3 (32158319)	T/C (T)	GWAS	0.860	0.811	3.86×10^{-10}	1.43	1.28–1.60	
				Validation	0.854	0.809	3.41×10^{-10}	1.38	1.25–1.53	
				Combined	0.856	0.810	8.38×10^{-20}	1.40	1.30–1.51	0.661
rs878860	*OR10A3-NLRP10*	11p15.4 (7968359)	A/G (G)	GWAS	0.603	0.540	3.47×10^{-10}	1.30	1.20–1.40	
				Validation	0.601	0.533	1.95×10^{-13}	1.32	1.23–1.42	
				Combined	0.602	0.537	1.54×10^{-22}	1.31	1.24–1.38	0.747
rs6780220	*GLB1*	3p21.33 (33087200)	T/G (G)	GWAS	0.582	0.539	1.55×10^{-5}	1.19	1.10–1.29	
				Validation	0.596	0.530	1.39×10^{-12}	1.31	1.21–1.41	
				Combined	0.590	0.535	2.77×10^{-16}	1.25	1.19–1.32	0.093
rs12634229	*CCDC80*	3q13.2 (112376308)	A/G (G)	GWAS	0.379	0.328	7.60×10^{-8}	1.25	1.15–1.36	
				Validation	0.391	0.326	8.18×10^{-14}	1.33	1.23–1.43	
				Combined	0.386	0.327	1.56×10^{-19}	1.29	1.22–1.37	0.303
rs4722404	*CARD11*	7p22 (3128789)	A/G (G)	GWAS	0.365	0.327	5.69×10^{-5}	1.18	1.09–1.28	
				Validation	0.362	0.325	2.67×10^{-5}	1.18	1.09–1.27	
				Combined	0.363	0.326	7.83×10^{-9}	1.18	1.12–1.25	0.911
rs10995251	*ZNF365*	10q21.2 (64398466)	T/C (C)	GWAS	0.568	0.518	7.73×10^{-7}	1.22	1.13–1.33	
				Validation	0.576	0.504	5.78×10^{-15}	1.34	1.24–1.44	
				Combined	0.572	0.511	5.85×10^{-20}	1.28	1.22–1.36	0.107
rs16999165	*CYP24A1-PFDN4*	20q13 (52807221)	T/C (T)	GWAS	0.729	0.691	3.87×10^{-5}	1.21	1.10–1.32	
				Validation	0.726	0.694	1.47×10^{-4}	1.17	1.08–1.27	
				Combined	0.728	0.692	1.65×10^{-8}	1.19	1.12–1.26	0.618

RAF, risk allele frequency; OR, odds ratio; CI, confidence interval.
[a]*P* values of the Cochran-Armitage trend test for each stage. [b]Results of combined analyses were calculated by the Mantel-Haenszel method. [c]Odds ratios and confidence intervals were calculated using the non-risk allele as a reference. [d]Results from the Breslow-Day test.

the validation set by the Mantel-Haenszel method, and a total of eight loci were found to be associated with atopic dermatitis at genome-wide significance (**Figs. 1** and **2** and **Table 1**). The Breslow-Day test showed an absence of significant heterogeneity ($P > 0.05$) (**Table 1**). We further assessed interactions among the eight newly discovered loci using the GWAS and validation data. We also conducted epistasis analysis, including the seven previously published loci, using the GWAS data. However, there was no evidence of an epistatic effect on susceptibility to atopic dermatitis with any combination of the 15 loci (**Supplementary Table 4**).

We obtained association results for >7 million imputed SNPs. In this study, a subset of genotype data for controls in the validation study was obtained from the GWAS data, but DNA samples were not available (**Supplementary Table 1**). Other cases and controls in the validation study were directly genotyped for SNPs at each locus. Thus, we focused on the directly genotyped SNPs in our GWAS and conducted a validation study. By imputation, we found that a total of 79 SNPs in 30 chromosomal regions were associated with atopic dermatitis at $5 \times 10^{-8} < P < 1 \times 10^{-4}$ (**Supplementary Table 5**). Further studies are needed to characterize the 30 regions suggested by imputation to associate with atopic dermatitis.

We next conducted conditional logistic regression analysis of the eight newly discovered loci using the GWAS data (**Supplementary Fig. 3**). This analysis indicated that there were two independent association signals in the MHC class I and III regions, one between *HLA-C* and *HLA-B* (rs9368677) and the other within *C6orf10* (rs9469099) (**Fig. 2a** and **Supplementary Fig. 3a**). In the *ZNF365* region, we observed independent signals at rs10995251, rs1444418 and rs10822056 (**Supplementary Fig. 3b**); however, the associations at rs1444418 and rs10822056 did not reach genome-wide significance when we combined the data from the GWAS and validation study ($P = 1.73 \times 10^{-7}$ and 1.15×10^{-4}, respectively). There were no independent signals in the other six associated regions (**Supplementary Fig. 3c–h**).

The associated region at 2q12 contains genes encoding the receptors of interleukin (IL)-1 family cytokines: *IL1RL1*, *IL18R1* and *IL18RAP* (**Fig. 2b** and **Table 1**). IL-1 family members are abundantly expressed in the skin[8]. IL1RL1, a component of the IL-33 receptor, is expressed by T helper type 2 (T_H2) cells and mast cells[9]. It has been reported that IL-33 is secreted in the damaged tissues of atopic dermatitis and promotes T_H2-type immune responses and the pathogenesis of atopic dermatitis[9]. The IL-1 receptor cluster region at 2q12 and the *IL33* region at 9p24.1 have also been identified as susceptibility loci by recent GWAS for bronchial asthma[10,11].

We found the most significant association with atopic dermatitis at rs176095 in the MHC class III region when we combined the data from the GWAS and validation study (**Fig. 2a** and **Table 1**). To our knowledge, this is the first finding of an association of atopic dermatitis with the MHC region at a genome-wide significance level. The MHC region is associated with a number of autoimmune diseases[12], and the involvement of autoimmunity in chronic inflammation in individuals with atopic dermatitis has been suggested[1]. Immunoglobulin E (IgE) antibodies against keratinocytes and endothelial cells are observed in serum specimens from subjects with severe atopic dermatitis[13].

The region of association at 11p15.4 includes two genes, *OR10A3* and *NLRP10* (**Fig. 2c** and **Table 1**). *OR10A3* is an olfactory receptor family gene, and *NLRP10* encodes a protein that belongs to the NALP protein family but lacks the leucine-rich repeat region. Individuals with atopic dermatitis are particularly susceptible to a number of microbial organisms, and pruritus is a major symptom of atopic dermatitis[1,2]. The itch-scratch cycle can lead to damage of the epidermal keratinocytes[1]. NLRP proteins are involved in sensing both microbial and danger signals[14], and NLRP10 has an anti-inflammatory

role through negative regulatory effects on caspase-1–dependent IL-1β secretion and apoptosis-associated speck-like protein containing a caspase recruitment domain (ASC)-mediated nuclear factor (NF)-κB activation[15].

The chromosome 3p21.33 region contains four genes, and the most significantly associated SNP, rs6780220, was located within *GLB1*, which encodes β-galactosidase-1 (**Fig. 2d** and **Table 1**). Notably, the associated region is located adjacent to the *CCR4* gene, which encodes a T_H2-associated chemokine receptor for CCL22 and CCL17 (also known as TARC). Keratinocyte-derived TSLP induces dendritic cells to produce TARC, and CCR4 mediates skin-specific recruitment of T cells during inflammation[1,16].

The associated region at 3q13.2 contains *CCDC80* (**Fig. 2e** and **Table 1**), which encodes a protein involved in the induction of C/EBPα and peroxisome proliferator-activated receptor γ (PPARγ)[17]. C/EBPα and C/EBPβ are coexpressed in basal keratinocytes and are upregulated when keratinocytes exit the basal layer and undergo terminal differentiation[18]. PPARγ acts as a negative regulator in immune cells, and a PPARγ agonist markedly suppresses both expression of thymic stromal lymphopoietin (TSLP) in the skin and maturation and migration of dendritic cells in a mouse model of atopic dermatitis[19].

The associated region at 7p22 contains *CARD11* (**Fig. 2f** and **Table 1**), which encodes CARMA1, an essential scaffold protein for lymphocyte activation via T-cell receptor (TCR) and B-cell receptor (BCR) signaling[20]. CARMA1 has an essential role in T-cell differentiation as well as a critical role in the regulation of the JunB and GATA3 transcription factors and the subsequent production of T_H2 cell–specific cytokines[21]. Mice that are homozygous for the mutation affecting Carma-1 show gradual development of atopic dermatitis with very high levels of serum IgE[22].

The region of association at 10q21.2 contains three genes, and the most significantly associated SNP, rs10995251, was located within *ZNF365* (**Fig. 2g** and **Table 1**). The region was reported to show suggestive association with atopic dermatitis ($P = 1.05 \times 10^{-7}$) by the previous GWAS of Chinese individuals[6], in which the association reached the genome-wide significance level. Notably, the region contains *EGR2*, which encodes a T-cell anergy-associated transcription factor that activates the expression of genes involved in the negative regulation of T-cell proliferation and inflammation[23].

The associated region at 20q13 includes *CYP24A1* and *PFDN4* (**Fig. 2h** and **Table 1**). *PFDN4* encodes a subunit of prefoldin, which is a molecular chaperone complex. *CYP24A1* encodes a mitochondrial cytochrome P450 superfamily enzyme. The protein initiates the degradation of 1,5-dihydroxyvitamin D3, the active form of vitamin D_3, by hydroxylation of the side chain[24]. Vitamin D is a modulator of innate and adaptive immune system functions[24], and an association between vitamin D deficiency and the severity of atopic dermatitis has been reported[25].

In this study, we identified variants at the *IL1RL1* and human leukocyte antigen (HLA) loci that associated with atopic dermatitis and replicated the associations at the *KIF3A-IL13* and *C11orf30* regions. The *C11orf30* region contains *LRRC32*, a gene previously reported to be specifically expressed in activated human naturally occurring regulatory T cells (nTreg)[26]. Atopic march is the natural history of atopic manifestations, and the clinical signs of atopic dermatitis generally predate the development of asthma and allergic rhinitis[27]. Recent GWAS have identified associations of the *IL1RL1*, HLA, *IL13* and *C11orf30* regions with bronchial asthma[10,11,28,29] and association of the *C11orf30* region with allergic rhinitis[30]. These findings suggest that atopic dermatitis and asthma or allergic rhinitis have overlapping susceptibility regions and that these regions contain common genetic factors for many allergic diseases. We stratified the cases by comorbidity of asthma and conducted an association study of asthma in the Japanese atopic dermatitis population for a total of 15 SNPs in the 7 previously reported and 8 newly identified regions. Notably, the most significant association was observed in the *IL1RL1* region ($P = 7.04 \times 10^{-9}$) (**Supplementary Table 6**).

In conclusion, we identified eight new susceptibility loci for atopic dermatitis at genome-wide significance, and we replicated the seven previously reported loci associated with atopic dermatitis in the Japanese population. Candidate genes at these loci suggest roles for epidermal barrier functions (*FLG* and *OVOL1*), adaptive immunity (*TNFRSF6B*, *IL13* and *CARD11*), IL-1 family signaling (*IL1RL1*, *IL18R1* and *IL18RAP*), negative regulation of apoptosis and the inflammatory response (*NALP10*), regulatory T cells (*LRRC32* and *EGR2*) and the vitamin D pathway (*CYP24A1*) in the pathogenesis of atopic dermatitis. Further studies are needed to better understand the genetic etiology and pathophysiology of atopic dermatitis.

URLs. The Leading Project for Personalized Medicine, http://biobankjp.org/; Haploview v4.2, http://www.broadinstitute.org/haploview/haploview; R statistical environment version 2.14.1, http://www.r-project.org/; minimac, http://genome.sph.umich.edu/wiki/Minimac; PLINK statistical software v1.07, http://pngu.mgh.harvard.edu/~purcell/plink/; LocusZoom, http://csg.sph.umich.edu/locuszoom/.

METHODS

Methods and any associated references are available in the online version of the paper.

Note: Supplementary information is available in the online version of the paper.

ACKNOWLEDGMENTS

We thank all the individuals who participated in the study and also thank the collaborating physicians for helping with sample collection. We are grateful to the members of BioBank Japan and the Rotary Club of Osaka-Midosuji District 2660 Rotary International in Japan for supporting our study. We thank M.T. Shimizu, H. Sekiguchi, A.I. Jodo, N. Kawaraichi and the technical staff of the Center for Genomic Medicine for providing technical assistance and K. Barrymore for proofreading this manuscript. This work was conducted as part of the BioBank Japan Project, which is supported by the Ministry of Education, Culture, Sports, Science and Technology, Japan. This work was also partly supported by grants from the Ministry of Health, Labour and Welfare, Japan.

AUTHOR CONTRIBUTIONS

T.H. and M.T. designed the study and drafted the manuscript. A.T. and T.T. analyzed the GWAS data. T.H., K.T., S. Tanaka and M.K. performed the genotyping for the GWAS. M.S., T.Y., S.F., S.D., A.M., T. Enomoto, C.N., N.N., K.M., S.I., K.O., H.O., E.N., T. Sakamoto, N.H., K.E., H.S., T. Sasaki, T. Ebihara, M.A., S. Takeuchi and M.F. recruited subjects and participated in the diagnostic evaluations. M.T. wrote the manuscript. M.K. and Y.N. contributed to the overall GWAS study design.

COMPETING FINANCIAL INTERESTS

The authors declare no competing financial interests.

Published online at http://www.nature.com/doifinder/10.1038/ng.2438.
Reprints and permissions information is available online at http://www.nature.com/reprints/index.html.

1. Bieber, T. Mechanisms of disease: atopic dermatitis. *N. Engl. J. Med.* **358**, 1483–1494 (2008).
2. Boguniewicz, M. & Leung, D.Y. Recent insights into atopic dermatitis and implications for management of infectious complications. *J. Allergy Clin. Immunol.* **125**, 4–13 (2010).
3. Palmer, C.N. *et al.* Common loss-of-function variants of the epidermal barrier protein filaggrin are a major predisposing factor for atopic dermatitis. *Nat. Genet.* **38**, 441–446 (2006).

4. Irvine, A.D., McLean, W.H. & Leung, D.Y. Filaggrin mutations associated with skin and allergic diseases. *N. Engl. J. Med.* **365**, 1315–1327 (2011).
5. Esparza-Gordillo, J. *et al.* A common variant on chromosome 11q13 is associated with atopic dermatitis. *Nat. Genet.* **41**, 596–601 (2009).
6. Sun, L.D. *et al.* Genome-wide association study identifies two new susceptibility loci for atopic dermatitis in the Chinese Han population. *Nat. Genet.* **43**, 690–694 (2011).
7. Paternoster, L. *et al.* Meta-analysis of genome-wide association studies identifies three new risk loci for atopic dermatitis. *Nat. Genet.* **44**, 187–192 (2012).
8. Johnston, A. *et al.* IL-1F5, -F6, -F8, and -F9: a novel IL-1 family signaling system that is active in psoriasis and promotes keratinocyte antimicrobial peptide expression. *J. Immunol.* **186**, 2613–2622 (2011).
9. Liew, F.Y., Pitman, N.I. & McInnes, I.B. Disease-associated functions of IL-33: the new kid in the IL-1 family. *Nat. Rev. Immunol.* **10**, 103–110 (2010).
10. Moffatt, M.F. *et al.* A large-scale, consortium-based genomewide association study of asthma. *N. Engl. J. Med.* **363**, 1211–1221 (2010).
11. Torgerson, D.G. *et al.* Meta-analysis of genome-wide association studies of asthma in ethnically diverse North American populations. *Nat. Genet.* **43**, 887–892 (2011).
12. Horton, R. *et al.* Gene map of the extended human MHC. *Nat. Rev. Genet.* **5**, 889–899 (2004).
13. Altrichter, S. *et al.* Serum IgE autoantibodies target keratinocytes in patients with atopic dermatitis. *J. Invest. Dermatol.* **128**, 2232–2239 (2008).
14. Magalhaes, J.G. *et al.* What is new with Nods? *Curr. Opin. Immunol.* **23**, 29–34 (2011).
15. Imamura, R. *et al.* Anti-inflammatory activity of PYNOD and its mechanism in humans and mice. *J. Immunol.* **184**, 5874–5884 (2010).
16. Vestergaard, C. *et al.* A Th2 chemokine, TARC, produced by keratinocytes may recruit CLA$^+$CCR4$^+$ lymphocytes into lesional atopic dermatitis skin. *J. Invest. Dermatol.* **115**, 640–646 (2000).
17. Tremblay, F. *et al.* Bidirectional modulation of adipogenesis by the secreted protein Ccdc80/DRO1/URB. *J. Biol. Chem.* **284**, 8136–8147 (2009).
18. Lopez, R.G. *et al.* C/EBPα and β couple interfollicular keratinocyte proliferation arrest to commitment and terminal differentiation. *Nat. Cell Biol.* **11**, 1181–1190 (2009).
19. Jung, K. *et al.* Peroxisome proliferator-activated receptor γ–mediated suppression of dendritic cell function prevents the onset of atopic dermatitis in NC/Tnd mice. *J. Allergy Clin. Immunol.* **127**, 420–429 (2011).
20. Hara, H. *et al.* Cell type–specific regulation of ITAM-mediated NF-κB activation by the adaptors, CARMA1 and CARD9. *J. Immunol.* **181**, 918–930 (2008).
21. Blonska, M. *et al.* CARMA1 controls Th2 cell–specific cytokine expression through regulating JunB and GATA3 transcription factors. *J. Immunol.* **188**, 3160–3168 (2012).
22. Jun, J.E. *et al.* Identifying the MAGUK protein Carma-1 as a central regulator of humoral immune responses and atopy by genome-wide mouse mutagenesis. *Immunity* **18**, 751–762 (2003).
23. Safford, M. *et al.* Egr-2 and Egr-3 are negative regulators of T cell activation. *Nat. Immunol.* **6**, 472–480 (2005).
24. Hart, P.H., Gorman, S. & Finlay-Jones, J.J. Modulation of the immune system by UV radiation: more than just the effects of vitamin D? *Nat. Rev. Immunol.* **11**, 584–596 (2011).
25. Peroni, D.G. *et al.* Correlation between serum 25–hydroxyvitamin D levels and severity of atopic dermatitis in children. *Br. J. Dermatol.* **164**, 1078–1082 (2011).
26. Wang, R. *et al.* Expression of GARP selectively identifies activated human FOXP3$^+$ regulatory T cells. *Proc. Natl. Acad. Sci. USA* **106**, 13439–13444 (2009).
27. Spergel, J.M. & Paller, A.S. Atopic dermatitis and the atopic march. *J. Allergy Clin. Immunol.* **112**, S118–S127 (2003).
28. Hirota, T. *et al.* Genome-wide association study identifies three new susceptibility loci for adult asthma in the Japanese population. *Nat. Genet.* **43**, 893–896 (2011).
29. Ferreira, M.A. *et al.* Identification of *IL6R* and chromosome 11q13.5 as risk loci for asthma. *Lancet* **378**, 1006–1014 (2011).
30. Ramasamy, A. *et al.* A genome-wide meta-analysis of genetic variants associated with allergic rhinitis and grass sensitization and their interaction with birth order. *J. Allergy Clin. Immunol.* **128**, 996–1005 (2011).